AN ABSTRACT OF THE THESIS OF

ROBERT EDGAR CHANEY (Name) for the DOCTOR OF PHILOSOPHY (Degree)

in CHEMISTRY (Major) presented on 10/22/70 (Date)

Title: DIPOLE RELAXATION EFFECTS IN DOPED POTASSIUM CHLORIDE BY THE DOUBLE CRYSTAL METHOD

Abstract approved: Redacted for privacy
W. J. Fredericks

The investigation of impurity effects on the properties of alkali halide crystals has often been difficult because of the variation of procedures used in various experiments. The purpose of this work is to develop a self consistent method of measuring the IV dipole polarization properties of single crystals while eliminating the effects of the electrodes and the host lattice in the temperature range of -50 to 0°C. This was done by applying Kirchhoff's rule to a circuit which included the sample being studied and a pure reference sample. By allowing the two crystals to charge and discharge in opposition, the effects due to IV dipoles can be separated from other relaxation processes in the samples. This is called the Double Crystal Method (DCM).

Investigations of high purity, OH^- free, potassium chloride doped with lead and cadmium yielded activation energies (ϵ) of $0.691 \pm .01$ ev and $0.636 \pm .01$ ev respectively for the reorientation

process of IV dipoles. This supports the theory of Dreyfus which predicts a decrease in ϵ with a decrease in impurity ion radius in the range of 0.9 to 1.4 Å.

The expected decrease in relaxation time constant (τ) with increasing temperature was observed to occur about 15°K higher in temperature than expected for the KCl:Pb^{2+} based on predictions from work reported in the literature. When samples of both KCl:Pb^{2+} and KCl:Cd^{2+} were heated in the presence of water vapor, changes in the relaxation properties were observed. For the KCl:Cd^{2+} system the interaction was very rapid and difficult to observe. Two separate relaxations were observed however in a sample which had been exposed to atmospheric water. The one occurring at lower temperatures had nearly the same properties as the DCM results for untreated samples. The data for KCl:Pb^{2+} were not separable into two definite processes, however; there were indications that the difference between the DCM and other work could be due to the presence of more than one species of dipole. It was concluded that differences in the pretreatment of the salt before crystal growth were responsible for these results and that the relaxation in the lower temperature range was due to the interaction of the impurity ion with OH^-.

The concentration of dipoles was increased by heating the samples and vacuum quenching in order to reverse the aggregation process and freeze the dipole concentration at an optimum value.

Dipole Relaxation Effects in Doped Potassium Chloride by the Double Crystal Method

by

Robert Edgar Chaney

A THESIS

submitted to

Oregon State University

in partial fulfillment of
the requirements for the
degree of

Doctor of Philosophy

June 1971

APPROVED:

Redacted for privacy

Professor of Chemistry

in charge of major

Redacted for privacy

Chairman of Department of Chemistry

Redacted for privacy

Dean of Graduate School

Date thesis is presented 10/22/70

Typed by Clover Redfern for Robert Edgar Chaney

ACKNOWLEDGMENTS

In the completion of a project such as this help and encouragement come from many varied sources. Each contribution has been significant in its own way. The author would like to thank all of those who helped.

Fellowships provided by the United States Department of Health Education and Welfare, the Tektronix Foundation and the Shell Foundation are greatly appreciated.

The author would like to thank Professor W. J. Fredericks for his educational and technical assistance. Research associates in the solid state group including W. A. Propp, C. A. Allen and J. Paul are due thanks for many stimulating discussions and suggestions over the years. The help of G. Allison in design and construction of the time delay circuit and in consultations has been invaluable. The author would also like to thank Donna Klentz for her work on the drawings for this manuscript.

A special thank you goes to my wife, Patricia and my family, for without their faith and confidence this work could not have been completed.

TABLE OF CONTENTS

LIST OF FIGURES

LIST OF TABLES

DIPOLE RELAXATION EFFECTS IN DOPED POTASSIUM CHLORIDE BY THE DOUBLE CRYSTAL METHOD

I. INTRODUCTION

Early Work

The correlation between the addition of divalent impurity ions and change in physical properties of alkali halide single crystals has been studied for many years. Dielectric relaxation and polarization phenomena resulting from impurities were observed by Breckenridge (1948, 1950). Since that time several methods have been used to study these properties. Dielectric loss measurements have been made by Jacobs and co-workers (1961, 1963, 1967). Miliotis and Yoon (1969), Friauf (1954), Haven (1953), Watkins (1959) and others. Dreyfus (1961) developed the dc polarization technique. More recently Bucci and Fieschi (1964), Bucci and Riva (1965) and co-workers have developed the Ionic Thermocurrent (ITC) method.

All of the methods of observing the dielectric relaxation in alkali halides are based on the reorientation of dipoles in an electric field. The nature of these dipoles is discussed more fully in Chapter II. The well known Debye theory of polar molecules was applied to the dielectric loss experiments in order to explain the observations. It was found, however, that data could not be clearly explained unless a

more complex theory was applied. The experimental observations indicated that more than a single type of dipole was present. Dreyfus (1961) then attempted to separate the various contributions to the relaxation by the use of low temperature dc methods. His results agreed quite well with the dielectric loss work of Watkins and Haven. His work indicated that more than one type of dipole was present and the favored configuration changed.

It has been difficult in the past to compare the experimental results obtained in various laboratories, because every experimenter has used different procedures, different starting materials and different techniques.

Purpose

It is the purpose of this work to develop a method of obtaining self consistent measurements of the dielectric relaxation of potassium chloride single crystals in a manner such that all effects are eliminated except those due to the intentionally added divalent impurity ions. By the application of Kirchhoff's rules spurious effects of crystal capacitance, thermal history and electrodes can be eliminated or reduced to negligible magnitude from experimental observations by a technique which will be referred to as the Double Crystal Method (DCM).

II. POLARIZATION THEORY

Dipole Formation and Concentration

When divalent cations are introduced into the alkali halide lattice they commonly occupy a cation lattice site, therefore it is called a substitutional impurity. Because this occurs a cation vacancy must be formed for each divalent impurity ion incorporated in order to maintain the electroneutrality of the crystal.

Thermally produced vacancies, both anionic and cationic, occur as the temperature increases. They are formed in equal numbers. A pair of isolated oppositely charged vacancies is called a Schottky defect. The concentrations of cationic and anionic vacancies are related by the following equilibrium expression, which is called the Schottky Product,

$$K_s(T) = (n_+)(n_-) = \exp(-g_f/kT)$$

where n_+ and n_- are the concentrations of the vacancies expressed in mole fractions, g_f is the Gibbs free energy of formation for a Schottky defect, T is the absolute temperature and k is the Boltzman constant. Beaumont and Jacobs (1966) determined that g_f is given by

$$g_f = 2.259\text{ev} - T(0.463 \times 10^{-3}\text{ev}/^\circ\text{K})$$

for pure KCl. At 200°K, $K_s(T)$ becomes 1.86×10^{-22}. In a pure crystal the concentration of positive ion vacancies would then be 1.37×10^{-11} mole fraction. In an imperfect crystal the most abundant aliovalent impurity will contribute n_i vacancies. If the most common aliovalent impurity is a divalent cation with a concentration of 10^{-6} mf, in this temperature range and below, n_+ is set by n_i and n_- is suppressed. As the temperature of a sample is lowered from the melting point, the electrostatic attraction between the excess positive and negative charges of the aliovalent cation and vacancy relative to the lattice overcomes thermal excitation. The aliovalent impurity and a vacancy can form a stable configuration which is usually called an IV complex. The complex thus formed may take several forms depending on the relative positions the cation and vacancy take in the lattice. As shown in Figure 1, a complex may be formed with the vacancy taking a nearest neighbor (nn), next nearest neighbor (nnn) or other more distant site. If a is the distance between K^+ and Cl^- sites, the complex bond distance will be $(\sqrt{2})a$, $2a$, $(2\sqrt{2})a, \ldots$ respectively. In the KCl lattice the nn complex has 12 equivalent orientations that it can take, the nnn complex is six fold degenerate and so on for each configuration of increasing bond distance.

The overall process of complex formation has been discussed by Lidiard (1957) and may be written as a quasi-chemical equation of

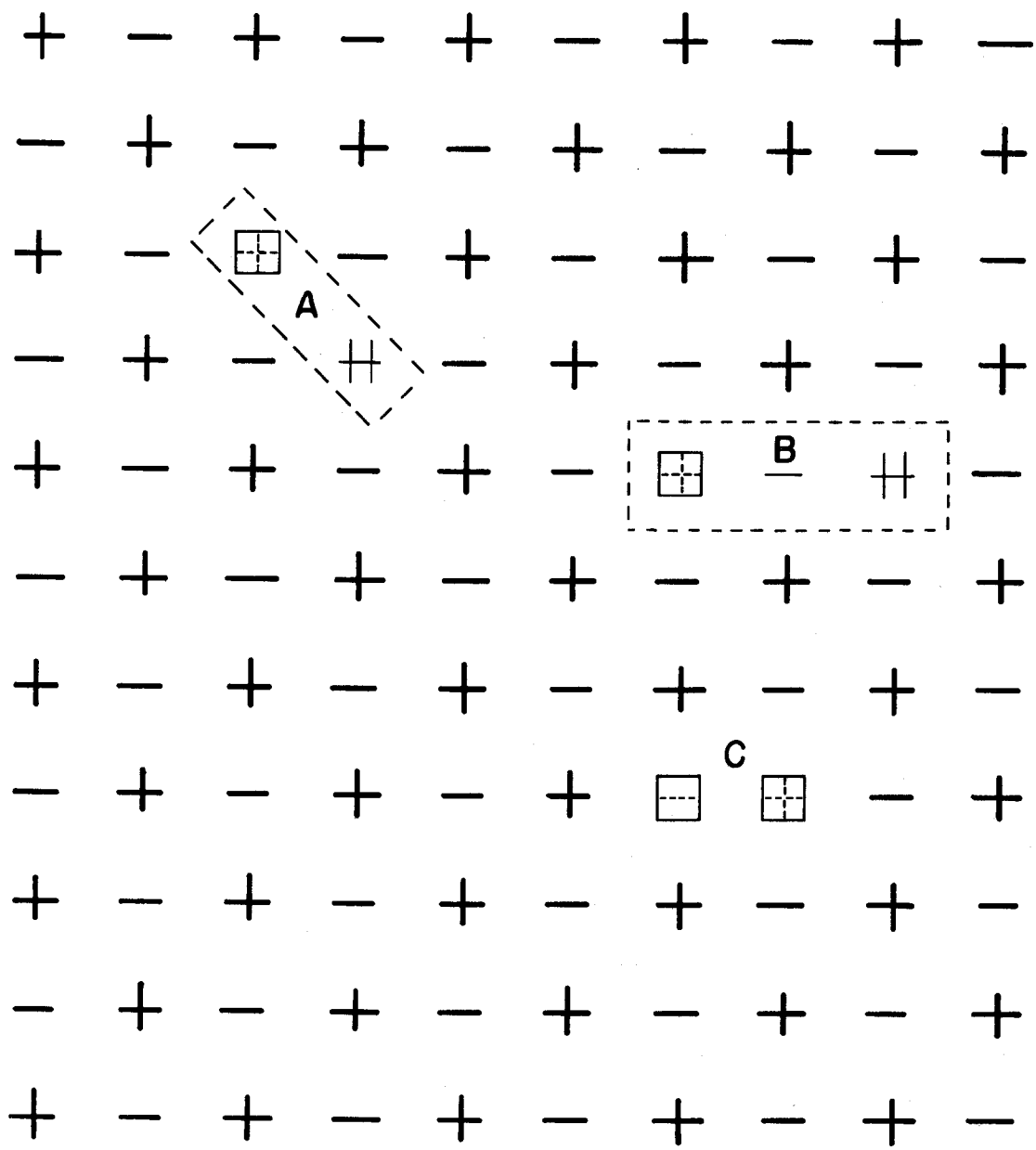

Figure 1. KCl lattice with imperfections: A) nn IV dipole, B) nnn IV dipole, C) Schottky vacancy pair (associated).

the form

$$M^{2+} + \text{vacancy} \rightarrow IV$$

where IV represents the impurity-vacancy complex. These complexes have a dipole moment arising from the concentration of charge at the impurity and the vacancy.

Keneshea and Fredericks (1963, 1964, 1965) have determined the free energy of association for the IV complex in $KCl:Pb^{2+}$ and $KCl:Cd^{2+}$ to be $0.48 \pm .01$ ev and $0.47 \pm .01$ ev respectively at 400° C. The equilibrium constant and degree of association for the chemical reaction above can be calculated at the quenching temperature used in this work by using the following equation from Lidiard (1957),

$$K = p/(1-p)^2 = z_1 c \exp(\zeta_1/kT)$$

where K is the equilibrium constant, p is the degree of association, z_1 is the number of equivalent orientations which the dipole can take in the KCl lattice, c is the mole fraction of divalent impurity ions present, ζ_1 is the free energy of association, T is the absolute temperature, and k is the Boltzman constant. The quenching temperature used is discussed in Chapter IV. It was 400° C. The degree of association at this temperature is 0.52 for $KCl:Pb^{2+}$ and 0.51 for $KCl:Cd^{2+}$ for crystals containing 50 ppm impurity ion concentration. At 300°K (room temperature) p is very nearly one

for both of these systems.

Dipole Aggregation

The dipoles can form clusters. If a crystal is slowly cooled from the melting point the impurity ions and vacancies are first dissociated, next complexed and below about 400° C the complex concentration reaches a maximum, then decreases as clusters or precipitates grow. Cook and Dryden (1962), Dryden and Harvey (1969), Cappelletti and DeBendetti (1968) are among those who have studied the aggregation process in the alkali halides.

If however a sample after being cooled to room temperature is heated to about 400° C for 1 hour and cooled by a relatively slow quench to room temperature the results of Dryden and Harvey indicate that almost all of the clusters are disassociated into dipoles which are "frozen" into the lattice. At room temperature the recombination process to form clusters is sufficiently slow that the concentration of IV dipoles is held at a maximum for about four days before recombination decreases the dipole concentration appreciably.

Properties of Dipoles in an Electric Field

The divalent cation has a charge of +1 and the vacancy has a -1 charge with respect to the lattice. When an electric field is applied to the crystal, the dipoles are oriented with respect to the field. The

current density within the crystal during this process can be described by

$$j = j_{\infty} + j_{o} \exp(-t/\tau) \tag{2.1}$$

where j is the current density, j_{∞} is the time independent current density at saturation, j_{o} is the initial current density due to the relaxation process, t is the time and τ is the time constant of the process.

When the field is removed, the current density expression for the reorientation of the dipoles is

$$j = -j_{o} \exp(-t/\tau) \tag{2.2}$$

where j_{o} is the initial decay current density which is the same as that in Equation (2.1). The time constant τ is related to the activation energy for the reorientation process ϵ, by

$$\tau^{-1} = A \exp(-\epsilon/kT) \tag{2.3}$$

where k is the Boltzman constant, T is the temperature in degrees Kelvin, ϵ is the activation energy, and A is a constant called the frequency factor. From the theory of Zener (1952) the constant A is given by

$$A = I\nu \exp(\Delta S/k) \tag{2.4}$$

where I is the number of similar jumps which a dipole may use to realign itself, ν is the vibrational frequency of the lattice and ΔS is the entropy change which occurs when a dipole is realigned.

Polarization of a Crystal in an Electric Field

When there is an electric field within a sample, the degeneracy of each dipole is removed causing one specific set of orientations to be favored, i.e., those orientations in which the dipole is as nearly as possible parallel with the field.

As outlined by Dreyfus (1961) the total polarization $P(\infty)$ observed in a system containing only one type of dipole is related to the current density $j(t)$ for the orientation process, the number of dipoles oriented Δn, and the dipole moment ae in the following manner

$$P(\infty) = \int_0^\infty j(t)dt = ae\Delta n \tag{2.5}$$

since

$$j(t) = j_o \exp(-t/\tau) \tag{2.6}$$

$$P(\infty) = \int_0^\infty j_o \exp(-t/\tau)dt = j_o\tau . \tag{2.7}$$

The total number of dipoles present N_n is related to the number oriented by the field E by:

$$\Delta n = \frac{N_n}{3}[\exp(Eae/kT) - \exp(-Eae/kT)]$$

$$\cong \frac{N_n}{3}(2Eae/kT), \qquad (2.8)$$

combining (2.5), (2.7) and (2.8) while eliminating $P(\infty)$ and Δn we obtain

$$N_n = 3k[\frac{j_o T\tau}{E}]/2a^2e^2 \qquad (2.9)$$

which indicates a method of determining the total number of dipoles N_n.

If there are more than one type of dipole in the sample the current density expression becomes

$$j(t) = \sum_n j_n \exp(-t/\tau_n) \qquad (2.10)$$

and

$$P(\infty) = \sum_n j_n \tau_n \qquad (2.11)$$

The Effect of Impurity Radius on Polarization

Dreyfus (1961) took the solutions of Lidiard (1957) for the polarization equations for dipoles in an ac field and adapted them to the dc field case for dipoles with jumps no greater than $2a$ from

the impurity ion. He found that the polarization, P(t), and the current density, j(t), were the sum of the two terms

$$P(t) = P_1[1-\exp(-\lambda_1 t)] + P_2[1-\exp(-\lambda_2 t)] \tag{2.12}$$

and

$$j(t) = dP(t)/dt = P_1\lambda_1\exp(-\lambda_1 t) + P_2\lambda_2 \exp(-\lambda_2 t) \tag{2.13}$$

where

$$P_1 = \frac{4(ae)^2 N_i E}{3kT(2+\omega_4/\omega_3)(\lambda_1-\lambda_2)} X[2(\omega_o+\omega_4)-\lambda_2(1+\omega_4/\omega_3)], \tag{2.14}$$

$$P_2 = \frac{4(ae)^2 N_i E}{3kT(2+\omega_4/\omega_3)(\lambda_1-\lambda_2)} X[\lambda_1(1+\omega_4/\omega_3)-2(\omega_o+\omega_4)], \tag{2.15}$$

and

$$\lambda_{1,2} = 2\omega_3 + \omega_o + \omega_4 \pm [(\omega_o+\omega_4-2\omega_3)^2+4\omega_3\omega_4]^{1/2} \tag{2.16}$$

where λ_1 and λ_2 refer to the + and - signs respectively in Equation (2.16). ω_1 is the jump frequency for the interchange between a nearest neighbor (nn) potassium ion and a nn vacancy. ω_2 is the jump frequency for the exchange of a divalent impurity ion and a nn positive ion vacancy.

$$\omega_o = \omega_1 + \omega_2 \tag{2.17}$$

ω_3 is for the motion of a next nearest neighbor (nnn) vacancy to nn site and ω_4 is for the exchange of a nn vacancy with a nnn

potassium ion. Dreyfus then discussed two limiting cases where the ω's could be separated.

Case I. Assuming $\omega_o \gg 2\omega_3, \omega_4$, then Equations (2.14), (2.15) and (2.16) reduce to

$$\lambda_1 \approx 2\omega_o + 2\omega_4 \tag{2.18}$$

$$\lambda_2 \approx 4\omega_3 \tag{2.19}$$

$$P_1/P_2 \approx \omega_3/\omega_4 \tag{2.20}$$

where Equation (2.20) is the ratio of the two relaxations. In Equation (2.18), λ_1 is the sum of all possible single jumps of a nn vacancy which can change the polarization. λ_2 is the sum of the jump frequencies for a nnn vacancy. P_1/P_2 is the ratio of the probabilities for a vacancy occupying a nn or nnn site. If the jump from one nn site to another is much more probable than any other the polarization has the characteristics of two relaxations caused by the redistribution of the nn and nnn vacancies.

Case II. If the approximation is made that $2\omega_3 \gg \omega_o, \omega_4$ then Equations (2.14), (2.15) and (2.16) now become

$$\lambda_1 \approx 4\omega_3 + \omega_4 \tag{2.21}$$

$$\lambda_2 \approx 2\omega_0 + \omega_4 \tag{2.22}$$

$$P_1/P_2 \approx \omega_4 + 4\omega_3 \tag{2.23}$$

Now λ_1 is associated with nnn vacancies and λ_2 with nn vacancies. In this case the λ associated with the faster relaxation (λ_1) describes the nnn type vacancies while in Case I the opposite is true. The ratio from Equation (2.23) is small however and the faster relaxation is not a major contributor to the polarization. In either case as long as ω_4 is small the relaxation can be separated into the nn and nnn contributions. If ω_4 is zero then only nn dipole relaxation will be observed as current decay described by a simple equation with a single exponential term. If ω_4 is larger than the other jumps then separation of the relaxations is not easily accomplished. By approximating the effects of impurity radius on each of the jump frequencies and comparing his results with that of Watkins (1959) and Haven (1953), Dreyfus concluded that divalent impurities in NaCl which have a radius greater than manganese (0.78 Å) can be described by Case II. Case I should apply for impurities smaller than manganese. For ions in the radius range of manganese and zinc there is a transition where neither case clearly applies. The very fast polarization predicted by Case I was observed only for the case of zinc.

In KCl the transition region should occur in the impurity radius range of 1.0 to 1.1 Å roughly 0.2 to 0.3 Å smaller than the potassium ion. This has been indicated by work done on KCl:Ba^{2+}, KCl:Sr^{2+} and KCl:Ca^{2+} systems.

In this work we have chosen Pb^{2+} and Cd^{2+} as the substitutional ions to use in KCl. These impurities have ionic radii which should give insight into the applicability of the Dreyfus theory.

III. THE DOUBLE CRYSTAL METHOD OF MEASUREMENT (DCM)

Time Dependent Current

As stated earlier many discrepancies have arisen in the literature as a result of the variation of experimental procedures from one laboratory to another. A way exists however, to isolate the effect of only the impurity in polarization measurements. Previously, as in the work of Dreyfus (1961), a pure crystal was run through the experimental procedure and the results of the doped sample were adjusted accordingly. This leaves some uncertainty about such factors as plating efficiency, thermal treatment and other physical differences in the samples as well as changes in the properties of the measuring circuit with time and manipulation.

If two crystals are charged or discharged so that the currents meet in opposition at a junction the resultant current flowing should be the difference in the two currents in accordance with Kirchhoff's rule.

By referring to Figure 2 it can be seen that crystal 1 and crystal 2 will contribute currents i_1 and i_2 respectively. The current flowing through the measuring device M will be $i_1 - i_2$.

If Z_1 and Z_2 are the impedances, including that of the samples, power supplies and measuring devices of the respective

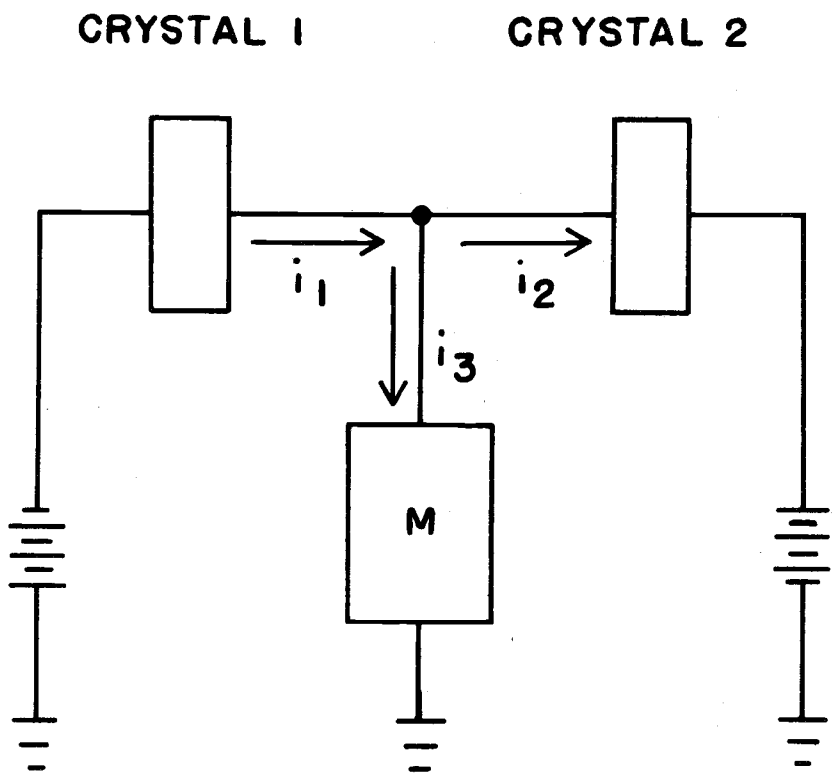

Figure 2. Schematic diagram of double crystal method.

branches, then the current of each branch (i_i) will be

$$i_i = (V_i/Z_i)\exp(-t/\tau_i) + i_{i\infty} \tag{3.1}$$

for charging and

$$i_i = -(V_i/Z_i)\exp(-t/\tau_i) \tag{3.2}$$

for discharging.

When a potential which is the same in magnitude, but of opposite polarity, $V_1 = -V_2$, is applied to each branch, the current flowing through the measuring device for charging becomes

$$i_m = (V_1/Z_1)\exp(-t/\tau_1) - (V_1/Z_2)\exp(-t/\tau_2) + i_{1\infty} - i_{2\infty} \tag{3.3}$$

and

$$i_m = (V_1/Z_1)\exp(-t/\tau_1) - (V_1/Z_2)\exp(-t/\tau_2) \tag{3.4}$$

for discharging.

If the circuit is arranged so that the two power supplies are replaced by one whose output terminals are maintained at a set voltage difference (V) the Equations (3.3) and (3.4) become

$$i_m = V/2\left[\frac{\exp(-t/\tau_1)}{Z_1} - \frac{\exp(-t/\tau_2)}{Z_2}\right] + i_{1\infty} - i_{2\infty} \tag{3.5}$$

for charging and

$$i_m = V/2\left[\frac{\exp(-t/\tau_1)}{Z_1} - \frac{\exp(-t/\tau_2)}{Z_2}\right] \tag{3.6}$$

for discharging.

In Equation (3.5), $i_{1\infty} - i_{2\infty}$ is a constant, independent of time. On a plot of current versus time this will appear as a straight line segment parallel to the zero current axis at long time, $t \gg \tau$. Since in this work we are concerned primarily with the time dependent portions of these curves, this straight line segment can be used as a base line. The time dependent portion can be separated by extending the $i_{1\infty} - i_{2\infty}$ line back to zero time and using it as the time axis for zero current. Since the time dependent portion of Equation (3.5) is identical with Equation (3.6), therefore either charging or discharging curves can be used to obtain information about the change in polarization current with time.

If each sample contributes a time dependent current which has a more involved form such as

$$i_{total} = i_{dipole} + i_{lattice} + i_{electrode} \tag{3.7}$$

then using the DCM the identical contributions of the crystals will add and subtract an equal amount to the measured current and thus isolate the time dependent current contribution which is produced by differences in the properties of the crystal capacitors. Some of these properties are discussed in the next section.

The Effect of Crystal Thickness Mismatch

One important factor to be considered in the DCM is the effect that a difference in crystal thickness can have on the current measured. If crystals 1 and 2 have the same surface area but thickness of 1.27 mm and 1.40 mm respectively, the discharge current which is recorded by the measuring device (an electrometer coupled to a recorder) from the application of 300 v to the system in Figure 2 is given by Equation (3.6). Neglecting other effects, if the resistor used in the electrometer is 10^{11} ohms and its input capacitance negligible, $Z_1 = Z_2 = 10^{11}$ ohms, $\tau_1 = C_1 \times 10^{11}$ and $\tau_2 = C_2 \times 10^{11}$. C_1 and C_2 can be calculated using

$$C = 0.224 \frac{\epsilon A}{d} \tag{3.8}$$

where ϵ is the dielectric constant, A is the electrode area and d is the crystal thickness. Guira and Spinolo (1968) have determined that $\epsilon = 4.86$ for KCl. A in our case is 1.98 cm^2. The thicknesses are given above. Applying Equation (3.8) gives $C_1 = 17.0$ pf and $C_2 = 15.4$ pf. This represents a 9.4% mismatch in thickness.

Equation (3.6) now becomes

$$i_m = 1.50 \times 10^{-9}[\exp(-t/1.70)-\exp(-t/1.54)] \tag{3.9}$$

Figure 3 shows the resulting current. Also shown is the result

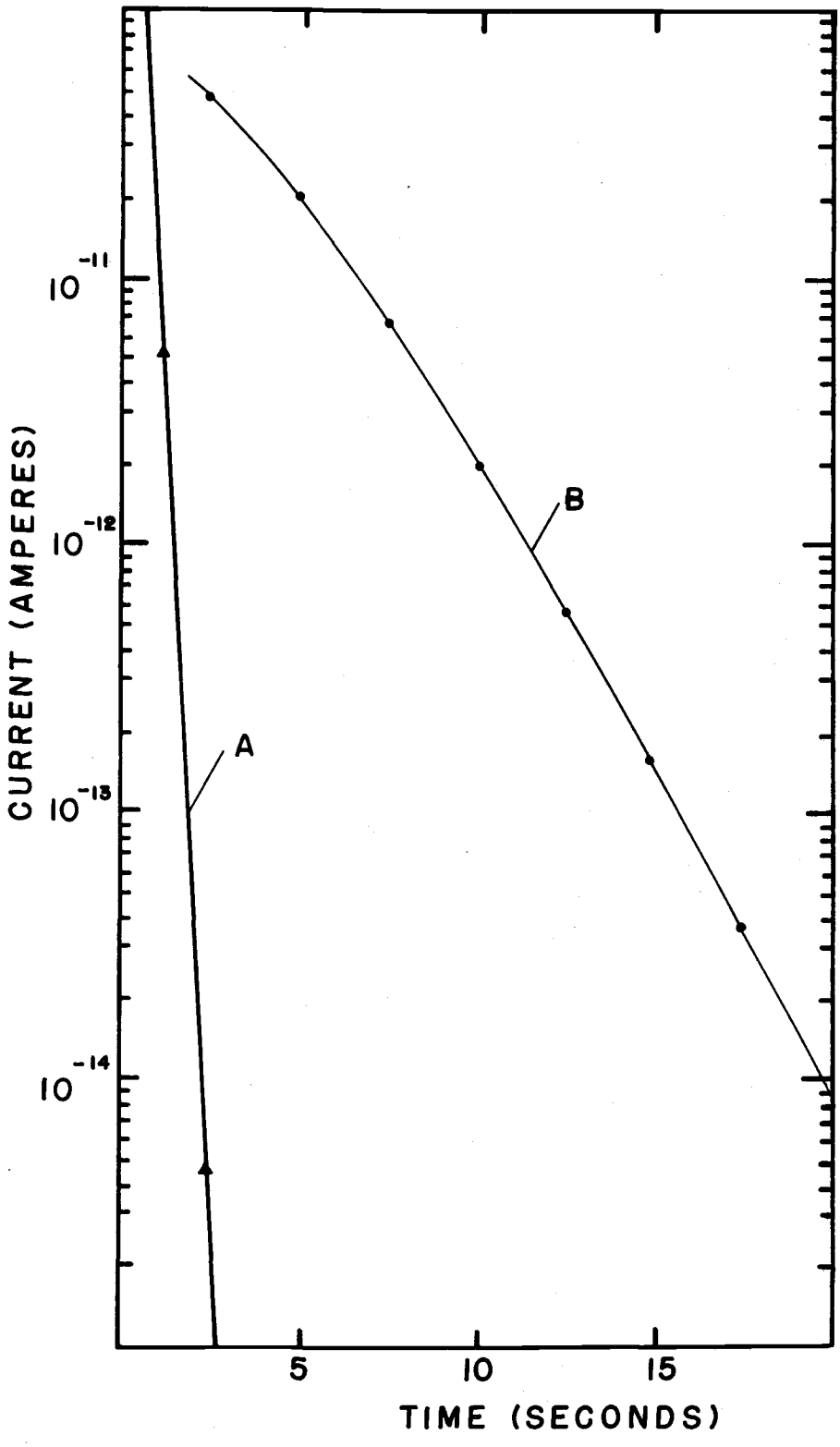

Figure 3. Current vs time-calculated for 9.4% crystal thickness mismatch: A) 10^{10} ohm shunt resistor, B) 10^{11} ohm shunt resistor.

of the same calculation based on the use of the 10^{10} ohm resistor in the electrometer.

Contribution of Plating, Dislocations and Effects Due to Sources Other than the Bulk Lattice

Sutter and Nowick (1963) and more recently Miliotis and Yoon (1969) have studied the effect of intentionally introduced air gaps between the sample and electrode on the polarization of alkali halide single crystals. They found that, as would be expected, the capacitance of the air gap and that of the crystal behaved as two capacitors in a series combination. Referring to Figure 4 it can be seen that the resulting combination will have capacitance C_T and R_T which are

$$C_T = \frac{C_1 C_2}{C_1 + C_2} \tag{3.10}$$

$$R_T = \frac{R_1 R_2}{R_1 + R_2} \tag{3.11}$$

The resulting time constant of the combination is

$$\tau = R_T C_T = \frac{(C_1 C_2)}{(C_1 + C_2)} \frac{(R_1 R_2)}{(R_1 + R_2)} \tag{3.12}$$

Sutter and Nowick using ac techniques in the temperature range 50°C to 200°C found that variation in the capacitance of the sample had

no effect on the resulting time constant and therefore did not consider it in their development. For that approximation τ is given by

$$\tau = \frac{C_2 R_1 R_2}{(R_1 + R_2)} \tag{3.13}$$

since $R_2 \gg R_1$

$$\tau \approx C_2 R_1$$

it should be noted that Sutter and Nowick used mica spacers which completely blocked the electrodes.

Miliotis and Yoon used a variation of this blocking technique to study the ac dielectric loss in the temperature range 200°C to 700°C. They introduced the air gaps by milling the center of the sample so that the corners, only about 10% of the surface, were in contact with the parallel plate electrodes. They found that much of their data could be explained by considering the sample's resistance and capacitance (R_s and C_s) and the capacitance of the air gap (C_A) in the arrangement shown in Figure 5. They found that the anamolus relaxations observed with no air gap could be eliminated by improving the electrode contacts and that the air gap method they used could explain some of the results they obtained with samples having poor electrode contacts or small air gaps between the electrodes and sample. To improve the contacts made by adding silver paint, they dried the paint

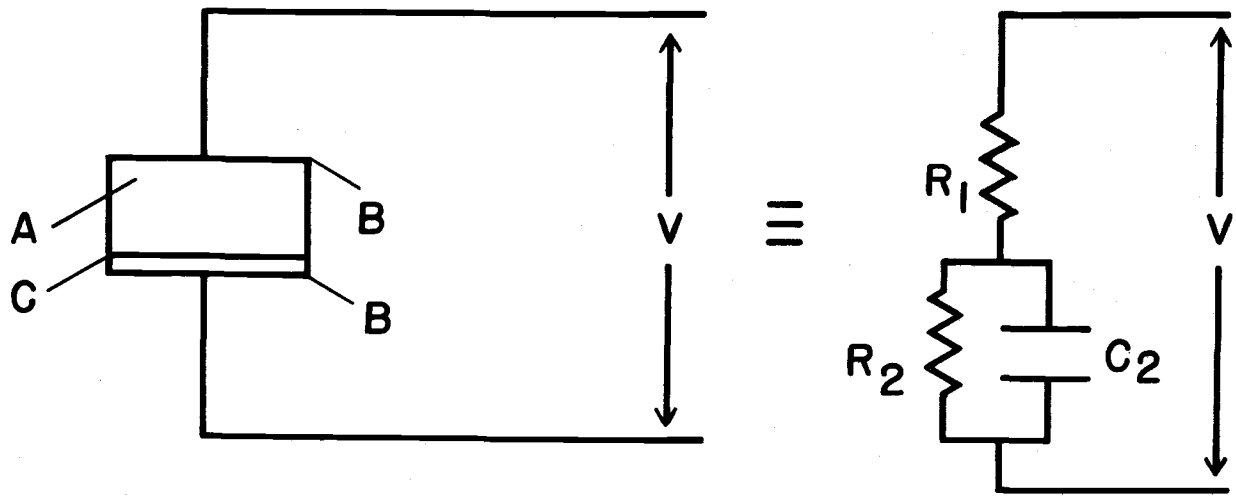

Figure 4. Resulting circuit of Sutter and Nowick (1963). A) sample, B) electrodes, C) mica spacer.

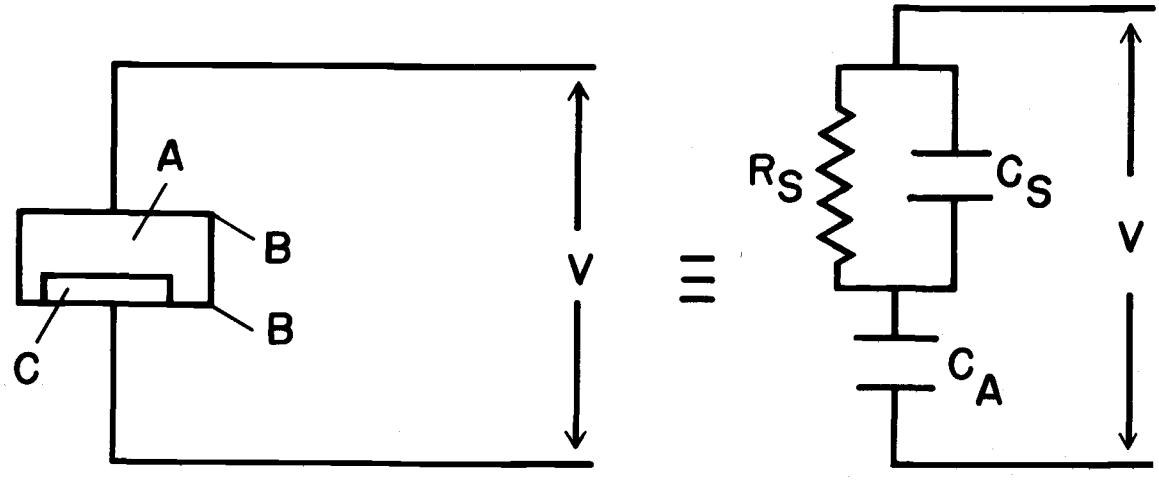

Figure 5. Resulting circuit of Miliotis and Yoon (1969). A) sample, B) electrodes, C) air gap.

slowly at room temperature for several days, then the samples were heated slowly to 200°C to further dry the electrodes. Then the samples were measured in the usual way. It should be noted, that while this surely did reduce possible air gaps due to the organic material in the paint, it also served to anneal the crystals and slightly reduce the numbers of dislocations present in the sample.

Figure 6 shows schematically two possible types of air gaps which can occur between a freshly cleaved crystal and a layer of plating or paint used for an electrode contact. Type (a) is caused by a small depression in the sample surface which can have several sources such as slip planes or jogs due to improper cleaving. Type (b) is a bubble of gas trapped during plating or painting. It may be air or perhaps organic solvent vapor from paint. In either type (a) or (b) the actual gap is small and the total surface area covered by each is much smaller than has been studied as in the work cited previously. If each air gap which is present has the properties of a capacitor then it should behave as if it were in a parallel rather than a series configuration with respect to that part of the surface junction which has no air gap. Thus these small imperfections in the coating should contribute to the total capacitance as capacitors in parallel. This would give a relaxation current of the form

$$i = A \exp(-t/\tau) \qquad (3.14)$$

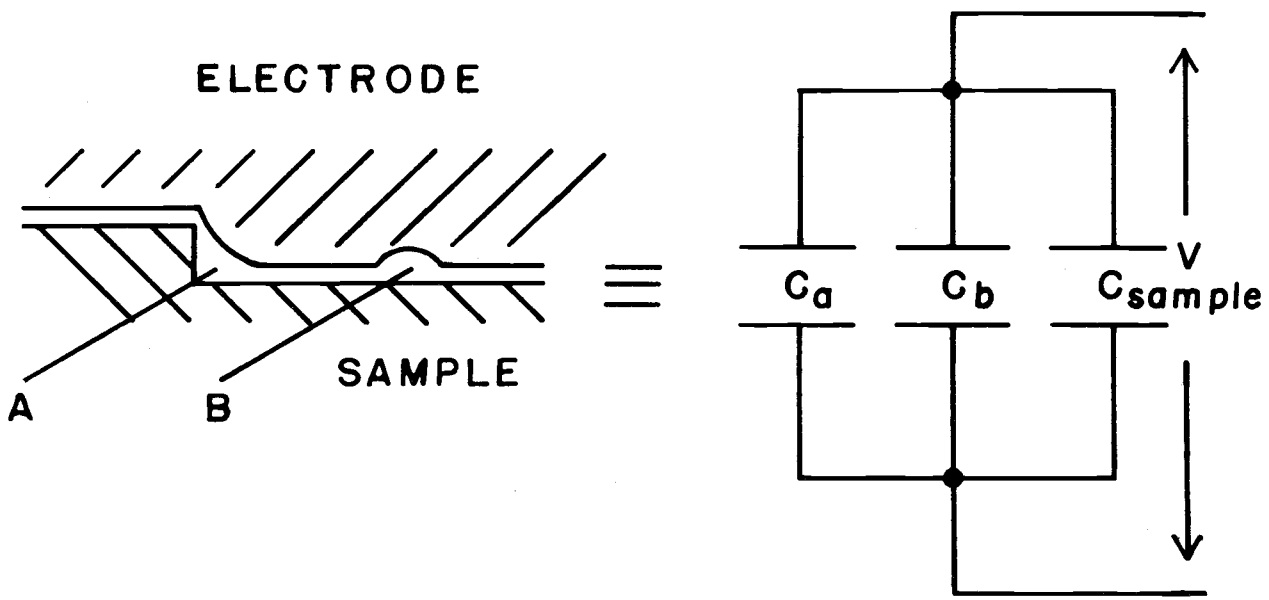

Figure 6. Some types of air gaps possible with their equivalent circuit: A) caused by step in surface, B) caused by trapped vapor or gas.

where

$$\tau = R_s(C_s+C_a+C_b).$$

Equation (3.14) is based on the assumption that the contribution of resistance of the air gaps had a negligible effect on the resistance of the total sample.

The work of Kao, Whitham and Calderwood (1970) has, however, shown that polarizations of long time constants in the range of 100 to 300°C can be described by a current expression involving the sum of exponentials.

$$i = A \exp(-t/\tau_a) + B \exp(-t/\tau_b) \qquad (3.15)$$

They concluded from their work that the relaxations which give rise to these terms were due to polarization processes involving dislocations and imperfections in the crystal lattice itself. If this is the case then it would be expected that these processes could be treated as if the dislocations were capacitors and the result could be expressed in terms of parallel capacitors. The current expression for a group of capacitors in parallel would then have the form

$$i = A \exp(-t/\tau) \qquad (3.16)$$

where

$$\tau = R_i \sum C_i.$$

Their experimental evidence however indicated that rather these systems behaved as current sources which are independent of each other and obey Kirchhoff's rule as in Figure 2, where

$$i_1 = i_2 + i_3 \tag{3.17}$$

and i_1 and i_2 can be expressed by simple exponential equations

$$i_a = A \exp(-t/\tau_a); \qquad i_b = B \exp(-t/\tau_b) \tag{3.18}$$

Dreyfus (1961) found that the polarization effects he observed in the temperature range -60 to 0°C could also be resolved by applying a similar relationship. The best fit was obtained by using the form

$$j = j_o \exp(-t/\tau_a) + \sum_i j_i \exp(-t/\tau_i) \tag{3.19}$$

where τ_a is the time constant related to the IV dipole relaxation involving nn or nnn vacancies and τ_i's were attributed to relaxations involving vacancies at further lattice sites. This also is an example of Kirchhoff's rule.

The assertion can then be made that since within the sample processes which might be expected to have the properties of capacitors in parallel, i.e., as in Equation (3.14), can be shown to obey a current expression derived from Kirchhoff's rule, then the surface effects when considered on a microscopic scale may also be described

by the same method. Thus the effect of electrodes and dislocation polarizations may easily be separated by using DCM to counter-balance these effects in similarly grown and treated crystals.

IV. EXPERIMENTAL

Measuring Circuit

Basic Circuit

The dielectric relaxation measurements were made using the system shown in Figure 7. The power supply was a Keithley Model 241 Regulated Power Supply which was selected because it would be connected using a floating ground. The voltage appearing between the output terminals can be set by a five switch divider and multiplier to five significant figures ±0.05% or ±0.15 v at 300 v. The voltage divider was used to maintain the two output terminals at an equal potential above and below the system ground respectively.

The cables for both the power supply and the electrometer leads were made using Transradio No. C33-T low capacitance coaxial cable. Connections were made to the high voltage relay system by adapting standard Amphenol (83-822) connectors to the cable by means of 3/4" copper tube soldered to the connector. The electrometer input lead was connected, by using a Transradio (NC12-1) plug and (PC1201) socket, to the input relay system. The cable used for the electrometer input has a calculated capacitance of 15 pf.

The electrometer was a Keithley Model 610A. This was used basically as an amplifer which provided a 10 mv output to the recorder.

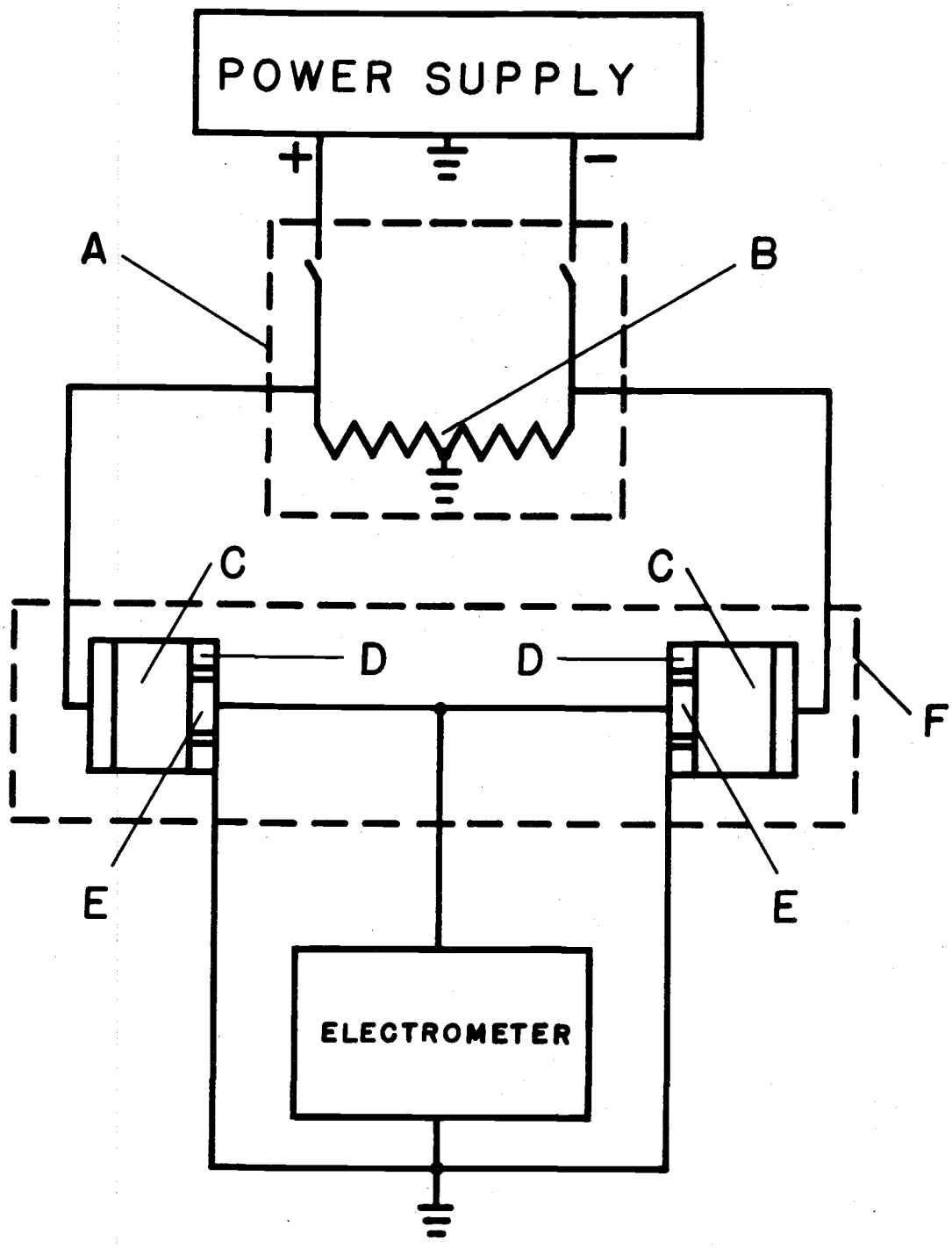

Figure 7. Schematic diagram of DCM: A) main switching assembly, B) voltage divider, C) samples, D) guard rings, E) electrodes, F) cell wall.

The electrometer was chosen because it has a feedback design which in low current ranges reduces the response time of the measuring circuit by 100. This feature is highly desirable because when measuring current of the magnitude of 10^{-12} amps a capacitance of 20 pf in the electrometer input leads can cause a response time constant of two seconds when using a 10^{11} ohm shunt resistor. A two second time constant due to instrumentation would require three or more times that length of time to obtain accurate current measurements from the signal source. By reducing the effective time constant the response of the circuit is increased to the point at which the response speed of the recorder is the limiting factor in the circuit's overall response. The recorder used was a Houston Instruments Model HR-98 X-Y recorder. The output of the electrometer was displayed on the Y axis and time was used as the X component employing the adjustable time sweep feature of the recorder. The sweep time of the readings was varied by changing the sweep rate of the recorder. The response time of the electrometer-recorder assembly is not more than 0.5 seconds for full scale deflection.

Switching Circuit

The switching circuit used for applying the field to the samples and triggering the electrometer input is shown in Figure 8. The

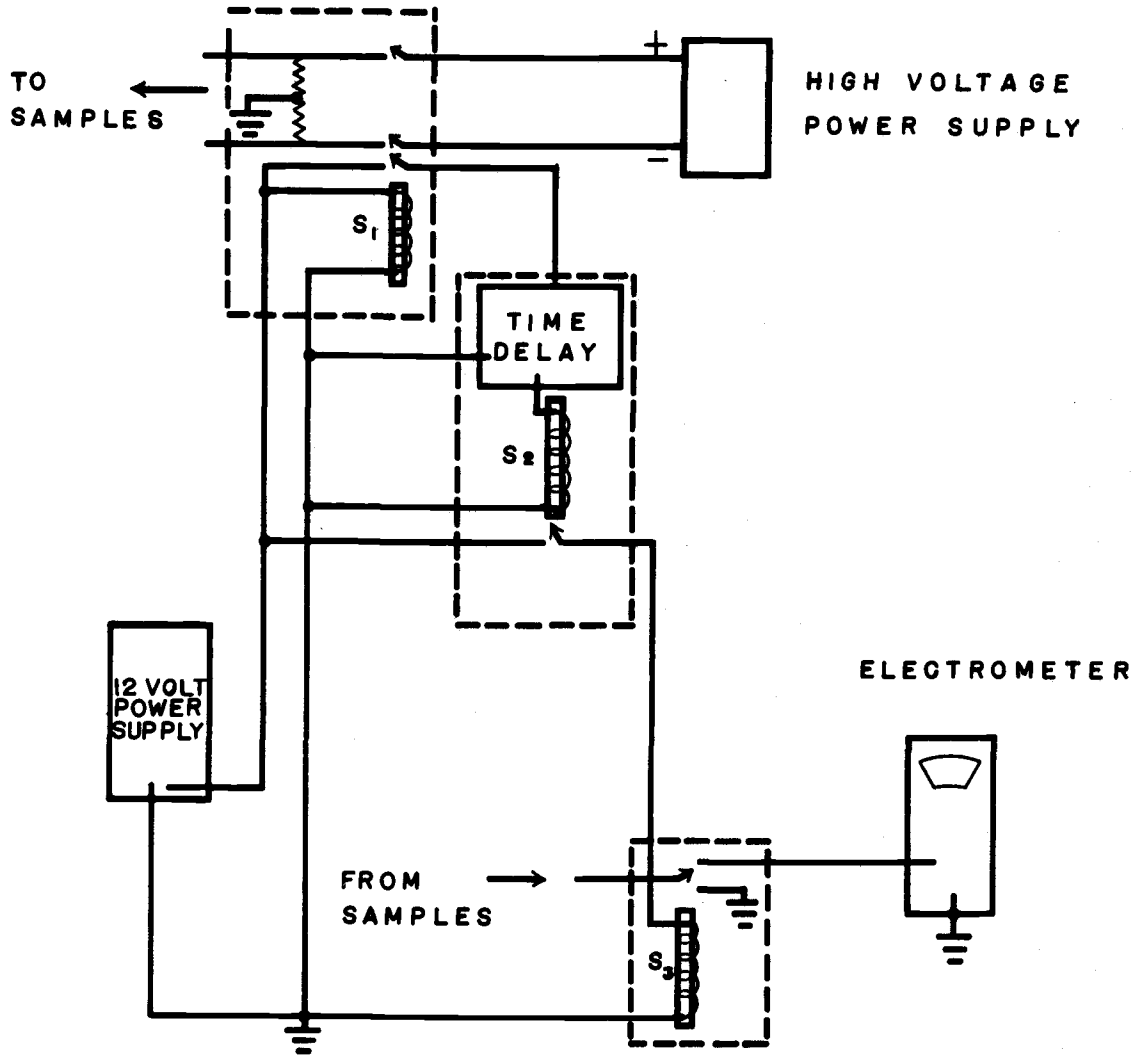

Figure 8. Schematic diagram of DCM switching circuit.

high voltage leads from the power supply are switched by means of Hamlin No. DRR-1-425 high voltage reed switches. These switches are manipulated by a 12 v solenoid (S_1) which is itself triggered by a toggle switch. Activation of the S_1 also triggers a time delay (TD) circuit. The purpose of this circuit is to provide a voltage which can be used to switch the electrometer input to the signal source after the initial surge of the signal from the lattice polarization of the samples has passed. This prevents overloading of the electrometer and distortion of the recorded signal.

A time delay of 0.33 sec was used. The slowest process in the dielectric behavior of a pure crystal is the ionic or lattice contribution. The application of a field to the crystal perturbs the normal vibrational properties of the sample and displaces the positive sublattice a fraction of a normal lattice distance in relation to the negative sublattice. The time required for this process, assuming instantaneous application of the field, should not be more than two or three times the vibration time of the lattice ions (10^{-13} sec). In the real case, the field is not applied to both crystals in the DCM at precisely the same instant. The switches fire within three milliseconds of each other. Therefore, the lattice polarizations were usually not entirely compensated and the current surge from the lattice polarization of the sample to which the field was last applied may have appeared at the electrometer input as much as three milliseconds

after the power switch was turned on. Due to the rapidly decaying nature of this contribution, even though the calculated polarization for this process is quite large for the samples used (~70 coul/cm^2), and the magnitude for the current spike is large, it is estimated that because of its expected rapid decay this effect will have dissipated from the measuring branch of the circuit in 10 to 20 milliseconds after the application of the field.

The voltage which is passed through the time delay circuit activates the solenoid of a normally closed relay (S_2). This breaks the circuit of a third solenoid (S_3) which operates the switching of the electrometer input. Initially this input is floating. When the solenoid is deactivated the imput is switched to the signal source. The lead from the samples is grounded when measurements are not being taken. This allows full discharge of the sample to ground. The power source used for all of the switching operations is a Heathkit Model 1P-20 Regulated Power Supply.

All of the circuitry used in the switching operations was enclosed in grounded metal cases to prevent stray pick-up by the electrometer imput. The ground of the switching circuit was the same as the measuring circuit.

Cryostat

The vacuum cell was designated in conjunction with W. A. Propp.

The original intent was to design a vacuum cryostat which could be used to make various types of low temperature electrical and optical measurements. The original lower section dimensions were determined so that it could be used in the Beckman DU, and Cary 14 spectrophotometers available at that time for optical measurements in this department. This section was made of stainless steel with vacuum tight ports for three quartz windows which allowed samples to be studied either by a single light path or by observation of emission at 90° to the light path.

The original bottom external section and sample holder were not large enough to conveniently hold samples of the necessary size, therefore, a different sample holder and envelope were built, as shown in Figures 9 and 10. The envelope is aluminum and the joints are slip O-ring seals.

The cold finger is attached to the crystal holder by means of a Teflon nut. Electrical insulation is achieved by inserting a Teflon wafer between the cold finger and crystal holder. This wafer must be thick enough so that the electrometer input signal is not shunted to the system ground. It was found that a Teflon wafer 0.2 cm thick was sufficient. The wafer also retards the cooling and warming rate of the sample holder. The cold finger and bottom of the cell's Dewar flask was made from a copper block. The rest of the Dewar and lower external flange assembly are stainless steel. The middle ring in the

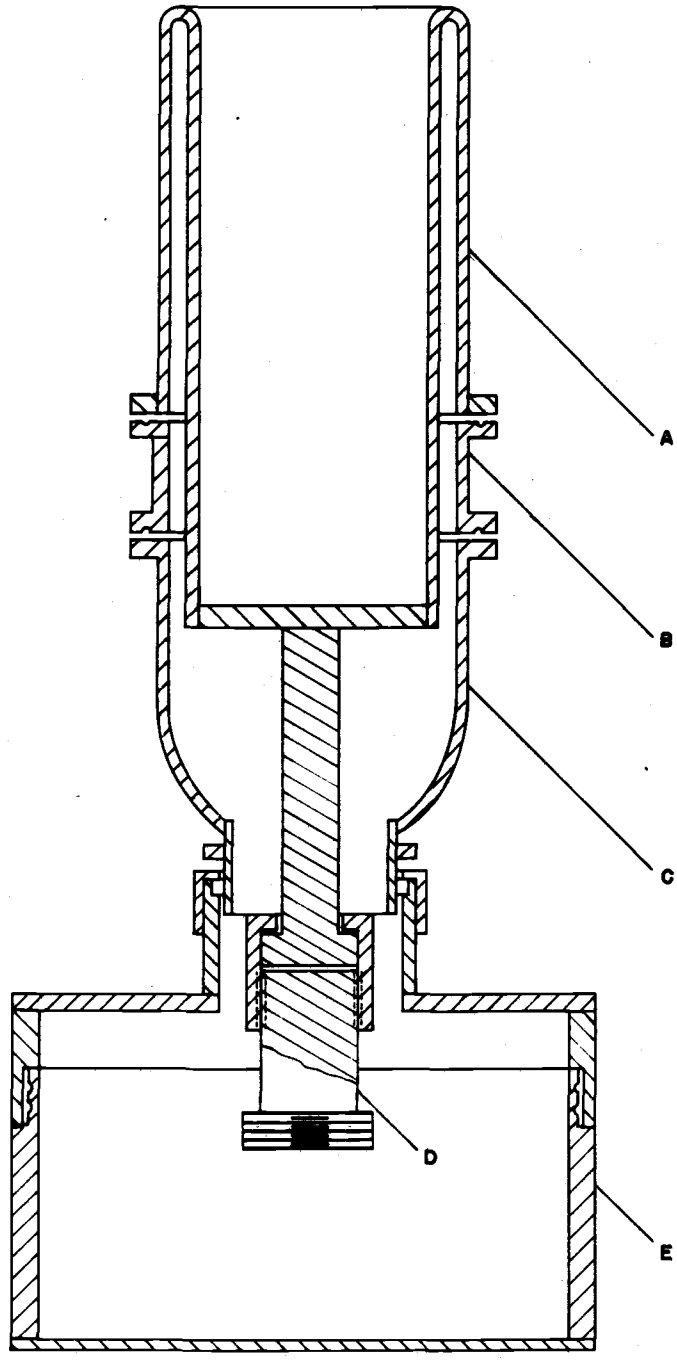

Figure 9. Cryostat: A) Dewar, B) brass ring, C) lower section, D) cold finger assembly, E) lower envelope.

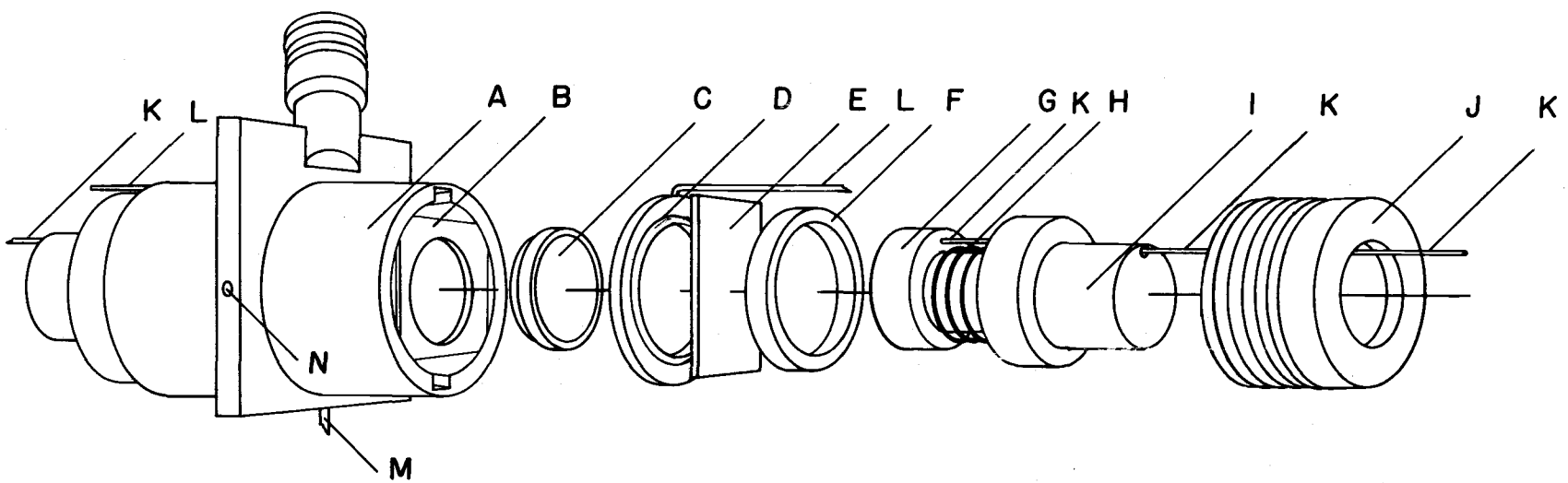

Figure 10. Exploded view of electrode assembly: A) sample holder with inside threads, B) Teflon electrode support, C) electrode with Teflon collar, D) guard ring with Teflon support, E) sample, F) Teflon washer, G) electrode, H) steel spring, I) Teflon plug, J) cap, K) high voltage leads, L) guard leads, M) electrometer lead, N) thermocouple well.

cell assembly is of brass. The flanges of the brass ring are sealed to the Dewar and lower assembly by means of O-ring seals held in place by steel bolts. This ring is fitted with two high voltage, two thermal couple, and six low voltage leads and the vacuum connection. The sample crystals were mounted in a massive copper crystal holder (Figure 10). The holder was made large in size to insure a slow temperature change of the crystals and to minimize thermal gradients. The holder and electrodes were gold plated to prevent corrosion. The electrodes themselves were supported by Teflon insulators where necessary.

The copper-constantan thermocouple is mounted in the thermocouple well (Figure 10) about 0.5 cm from each sample. Copper connection blocks were mounted on the sample holder. They were insulated from the holder by Teflon. The thermocouple calibration showed that the temperatures read were accurate to within ±0.5°C.

The thermocouple was checked after it was mounted in the cryostat by placing a second calibrated thermocouple between the copper electrodes and comparing the temperatures read on the two thermocouples as the cryostat was warmed up from -40°C. Even at a fast warming rate of 1°K per min, the thermocouple readings agreed well within the experimental error of ±0.5°C.

The cell when evacuated is capable of holding sample temperatures as low as -100°C. The minimum temperature possible varies

inversely with the thickness of the Teflon wafer. The cells warming rate can be controlled to about 40°C in 8 hours or less with addition of small amounts of liquid nitrogen. It can be held at an intermediate temperature ±2°C for about 2 hours, again if liquid nitrogen is judiciously added to the dewar. Measurements were made as the cell warmed slowly so that the temperature of the samples in the holder were as nearly as possible at an equilibrium thermal state. The thermal couple readings were made with a Leeds and Northrup Model No. 8686 potentiometer using the room temperature reference junction of the potentiometer.

Crystal Preparation

Salt Preparation and Treatment

The crystals used in this investigation were grown by the Kryopoulos technique. The method consists of melting the salt, lowering a single crystal seed into contact with the melt and slowly withdrawing the seed while allowing the KCl to freeze onto it, thus forming a large single crystal. This technique has been described by Patterson (1962).

The salt used for sample preparation was Merck reagent grade potassium chloride. This was then further purified by dissolving the salt in deionized water to make a concentrated 20% solution. This

solution was then filtered and passed through two ion exchange columns. The first column contained Chelex 100 (Bio-Rad analytical grade resin, 50-100 mesh) in the potassium form which removed heavy metal as well as alkaline earth cations. The solution was next passed through an anion exchange column which contained AG 2-X10 (Bio-Rad analytical grade resin, 50-100 mesh) in the chloride form. This resin removed such ions as I^-, NO_3^-, and Br^- as well as divalent anions. The solution was then evaporated to dryness to obtain the pure salt. This process is described by Fredericks, Schuerman and Lewis (1966). After complete treatment (see below) and crystal growth the salt contained about 20 ppb (molar) heterovalent cations.

Pretreatment of the salt just prior to crystal growth consisted of two separate steps. First the jacket was evacuated and the salt was heated at about 300°C for 8 to 12 hours to remove water from the salt or adhering to the quartz. Then a one-third atmosphere of dry HCl was introduced as the salt was heated to melting. This atmosphere contained a small amount of Cl_2 and was changed at least three times during the melting with the final charge remaining in the apparatus during the actual growth process. The HCl acts as a drying agent and removes hydroxide ion from the salt.

The divalent impurities were added as the chlorides to the salt before pretreatment. The $PbCl_2$ and $CdCl_2$ were reagent grade Baker and Adamson salts.

Growth Apparatus

A pulling assembly was built to grow the crystals for this work. The frame which supports the growth apparatus is made of Unistrut materials. The furnace shelf rests on a Unistrut support and is made of a quarter inch thick transite sheet. The outer shell of the furnace is a large clay flower pot. The inner shell is made from two Kanthol type 406 clam shell furnace elements. Each element is rated for 800 watts at 115 volts. The heating elements were wrapped with heavy aluminum foil to reduce radiant heat losses. Two cylindrical aluminum shields were placed between the elements and the outer shell and packed with vermiculite. Three cone shaped aluminum foil shields were sealed into place at the top of the furnace with alternating layers of moistened heavy asbestoes sheets. The bottom of the flower pot was covered with alternating discs of foil and asbestos.

The General Electric electronic grade quartz crucibles used to hold the melt were placed inside a quartz jacket four inches in diameter. They rested on a quartz cylinder 2" in diameter and 4" high. This raised them into the hottest part of the furnace. All quartz parts of the apparatus were cleaned by washing with Labtone and deionized water. They were then treated with hot nitric acid, thoroughly rinsed with deionized water and dried in a drying oven at 110°C. The tube was sealed at the lower end and was capped with a Monel

plate. The top of the tube is inserted into a Teflon ring which serves as an O-ring seat. The O-ring is then compressed by an aluminum nut, which screws into the bottom of the plate completing the seal. The plate is fitted with two gas ports and the cold finger feed-through seal. The seal is made from alternating three Teflon rings and two rubber O-rings seated into the top of the plate assembly with a nut.

Water is circulated through a quarter-inch copper tube coiled and pressure fitted to the plate. This provides cooling to the plate and protects the seals from excessive heating.

The Monel cold finger is rotated and raised or lowered by a pulling assembly designed by W. J. Fredericks and built by the OSU physics shop. The pulling assembly is controlled and regulated by a SA-12 Motor Speed Control Box from B & B Motor & Control Corporation. The pulling assembly is bolted to the slotted Unistrut frame so that it can be moved along a vertical track to facilitate manipulation of the apparatus. These bolts on the puller are the only rigid points of contact in the apparatus. The furnace rests on an asbestos mat on the shelf. The tube rests inside the furnace. The top plate is kept from riding up on the cold finger by pressure from an Unistrut angle, but otherwise it is not rigidly held. This allows the seal to seat between the cold finger and plate without forcing.

The first few pure crystals which were attempted were discarded because the Monel Screw and cold finger corroded. The

$HCl-Cl_2$ atmosphere appeared to attack the Monel even after attempts to eliminate all traces of water from the growth chamber. It was thought that the cool surfaces of the cold finger might condense any small amounts of water vapor which might be present in the salt even after the HCl treatment. The product of the corrosion was a brown scale on the metal surfaces. This changed to a light green compound after exposure to atmospheric water. The scale is believed to have been nickle chloride in various states of hydration. Subsequently the cold finger and seed holding screw used were Rhodium plated to prevent this corrosion.

The unit was connected to gas and vacuum lines through a single branch from an existing vacuum system. This arrangement provided for Cl_2 or HCl growth atmosphere. While changing the corrosive atmosphere, the gas was vented into a water aspirator. A liquid nitrogen trap was used to prevent water vapor from the aspirator from backing up into the growth chamber. All vapors from the growth chamber were either passed through the aspirator trap or a liquid nitrogen trap between the furnace and the vacuum line fore pump. The liquid nitrogen traps condense the HCl and Cl_2 so the latter trap was vented to the aspirator and both traps were warmed slowly to room temperature to remove the frozen gases and prevent possible damage to the pump.

The water used to cool the plate and the cold finger was piped

through a system made from half-inch copper tubing. The final connections to the plate and cold finger were made 1/4" id tygon tubing to provide flexability.

This system was used to grow the pure KCl and KCl:Pb^{2+} crystals used in this work. The KCl:Cd^{2+} crystals used were grown by a similar procedure in an apparatus described by Holmes (1966, p. 21-39). The growth process was slightly different than discussed previously in that during the growth of the crystal a constantly changing atmosphere of dried argon at atmospheric pressure was in the chamber.

The system of growth used produces crystals which are free of hydroxide. Each pure crystal was checked for hydroxide by observing the IV absorption spectrum. The OH^- in KCl absorbs at 204 nm. The whole crystal with the ends cleaved off was used as a sample. This provided a long path length and allowed small concentrations of OH^- to be observed. No OH^- was found in any of the pure crystals tested. However in the case of doped crystals this is not a reliable test for OH^-. Fritz et al (1963), Hattori et al (1967) and Allen (1969, p. 56, 89) have shown that divalent cations strongly interact with OH^-. The characteristic absorption of OH^- does not appear unless the concentration of OH^- exceeds the concentration of the M^{2+}.

After growth the crystals were annealed by placing them in the growth assembly and heating them to about 550°C and slowly cooling

them by changing the furnace settings over a period of 10 to 14 hours.

Electrode Plating

The samples were cleaved with a clean razor blade into samples of the desired size (2.5 cm x 2.5 cm x 1.3 mm). After quenching and spectral measurements, gold electrodes were vacuum evaporated onto the freshly cleaved or prepared surfaces.

The gold was cut from a thin sheet into small strips and suspended on a molybdenum filament which was heated by an ac power source. The filament was made of six strands of .004" molybdenum wire. The evaporation apparatus has been described by Seevers (1968, p. 28-31).

One side of the crystal was fully covered. The other side had a solid center circle of gold surrounded with a bare ring. Outside the bare ring, the rest of the surface was covered with gold. After being plated the edges of the sample were trimmed away to prevent shunting of the current. This electrode arrangement allows the use of a guarded measuring circuit.

Sutter and Nowich (1963) and Miliotis and Yoon (1969) have noted that the properties of electrodes vary from sample to sample. Three different methods of electrode preparation were used in this work. First freshly cleaved samples were gold plated as described above. It has been reported by Seevers and Scott (1970) that this type of

electrode is often non-ohmic and can cause serious polarization effects as described in Chapter II. The second method consisted of lightly sanding the surface prior to plating. This was done by using fine crocus cloth. While this method improves the ohmic character of the contacts, it causes distortion of the surface allowing the trapping of air bubbles and causing a large amount of polarization. The third process is an extension of the first. After electrodes were deposited on a sample with freshly cleaved surfaces, the sample was heated in a vacuum, and placed in a furnace for eight minutes at 400° C. It was then quenched to room temperature. This process sets the plating apparently by allowing the diffusion of the gold a short distance into the crystal as discussed in Chapter V for the prolonged heating of plated crystals at 400° C. This process decreases the spurious polarization effects and establishes ohmic contacts.

Quenching Techniques

In order to insure the maximum number of IV dipoles, each sample was moderately heated and quenched to room temperature. The apparatus used is shown in Figure 11. The outer tube is made of three different materials. The top section is made of Pyrex which has a large O-ring seal at the top. This connected to a Pyrex middle section which is in turn sealed to the quartz bottom. The Pyrex to quartz seal was obtained commercially. The experiments required

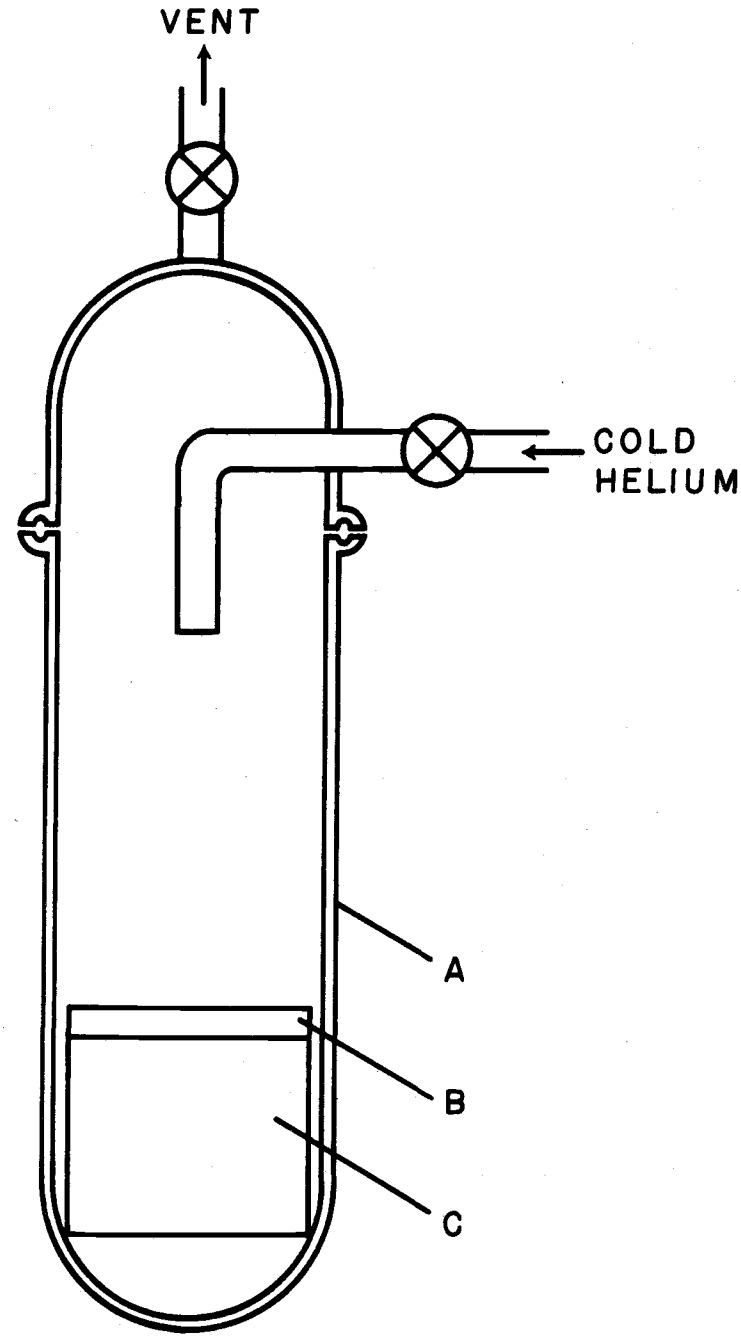

Figure 11. Quenching apparatus: A) Pyrex to quartz joint, B) platinum foil, C) stage.

that the tube be able to withstand thermal shock, but also required an O-ring or similar seal to facilitate repeated use. Therefore, this arrangement was used. The cap for the quenching tube is made of Pyrex and is fitted with two vacuum stop cocks.

The sample to be treated is placed on a platinum foil covered quartz stage and is lowered into the tube. The apparatus is evacuated and a small furnace is raised to surround the quartz section of the tube. After the heat treatment is completed, the furnace is removed and with He flowing, the tube is plunged into an ice bath. This process allows quenching from 400°C to room temperature in not more than two minutes. When the quenching process is complete, the tube is filled to slightly less than one atmosphere with He, sealed, removed from the vacuum system and allowed to equilibrate at room temperature before it is opened.

The He is cooled by passing it through a copper coil which is in a liquid nitrogen bath. The coil is made from ten feet of 3/8" copper tubing.

This process is similar to that described by Dryden and Harvey (1969). The temperature to which the samples were heated was 400°C. This temperature was decided upon because of the work of Dryden and Harvey concerning the aggregation processes of IV dipoles in alkali halides. They found that the maximum number of dipoles in a sample was obtained by heating the sample to about 400°C and quenching to

room temperature as described here. The optimum temperature for this procedure varies with the impurity present in the sample, but 400°C has been found to be a satisfactory temperature for this process.

Polarization Measurements

The samples for each polarization run were placed in the sample holders as soon as possible after the plating-quenching operation. The cryostat was then evacuated and out-gassed when necessary. The cell was left on the vacuum line until the pressure was $\leq 10^{-6}$ torr. In most cases the pumping operation was allowed to continue over night. The cell was then cooled, while still attached to the vacuum line, with liquid nitrogen until the temperature of the samples was lowered to the desired level. The cell was then sealed, moved to the measuring room and connected to the measuring circuit.

The polarization curves were then run as the sample holder slowly warmed to room temperature. After each polarization curve was recorded several minutes were allowed for the total discharge of the system before beginning the next measurement.

It was found that when pure samples of equal thickness (±1%), with electrodes prepared by the quenching technique were run through this procedure there were no indications of polarization effects anywhere in the temperature range covered from -50°C to room

temperature. It was found that the charging and discharging polarization curves showed no difference as predicted, therefore the polarization curves used for most of the subsequent work were taken while the samples were charging.

The electrometer-recorder system was checked by applying a known potential across standardized Victoreen Hi-Meg resistors and comparing the readings on various scale settings. The results were well within the electrometer specifications of ±4% of the full scale setting.

Checks were made for system noise during measurements by making traces with zero applied voltage. Some switching noise was picked up by the electrometer input, but this caused an initial current spike of short duration which was reproducible and could easily be corrected.

The recorder sweep rate was set at five seconds per centimeter and was checked periodically during the measurements. It was not found to vary more than ±2 mm for a 120 second sweep of 0.9%.

The measurements were made in a shielded room. It originally was used as a safety room for high pressure work. Its thick solid walls covered with steel plate provided isolation from spurious signals.

The limits on the values obtained experimentally were determined by means of standard error propagation techniques.

All calculations and least squares analyses were carried out on a Hewlett Packard 9100A calculator.

Analysis of Samples

The crystal samples used in this work were analyzed for lead and cadmium by polarography. Absorption spectroscopy was used in an attempt to determine the approximate doping level for KCl:Pb^{2+} before the samples were plated.

The polarographic analysis was conducted on a Heath EUW-401 system. The salt analyzed by this method was taken from the sample itself, from sections of the same boule slice or from the boule slice cleaved from one of the crystal surfaces when DCM sample preparation was taking place. The polarographic samples were weighed on a Mettler Type H-15 pan balance to the nearest milligram and dissolved in deionized distilled water. The solutions were made up to approximately 0.1 N KCl. With these solutions it was possible to determine impurity ion concentrations as low as $1.0 \times 10^{-6} \pm 0.2 \times 10^{-6}$ M which corresponds to 10^{-5} mole fraction or 10 ppm in the crystal sample.

Both cations have well defined polarographic waves which occur at potentials which are separated from the other characteristic waves of the system thus making lead and cadmium particularly suited for this method of analysis. The half-wave potentials of lead and cadmium are -0.40v and -0.6v respectively in 0.1 N KCl.

Each polarogram was made using a 25.0 ml portion of the unknown solution and 1.0 ml of 0.25% gelatin solution which was used as a maximum suppressing agent. The final gelatin concentration was 0.01%. Because of the dilution, the concentration of metal ion in the unknown solution was 1.04 times greater than that determined from the polarogram. All solutions were made with deionized distilled water.

Calibration curves for the polarograph were taken over the range of 10^{-3}M to 5×10^{-7}M concentration using solutions of known impurity concentration. The divalent metal ion concentration was determined by comparing the measured current at the half-wave potential with the calibration curves. With this information and the crystal sample weight the impurity concentration in the sample can be calculated.

The polarograph is rated at 1% accuracy with respect to the current imput from the dropping mercury electrode. However, it was found that for solutions of low concentration, the reproducibility was not as good as expected. At moderate concentrations of divalent metal ion the concentration measured is estimated to be within ±10% of the actual concentration. The absorption spectra of the samples were taken before plating on a Perkin-Elmer 450 spectrophotometer available in this laboratory. For the KCl:Pb^{2+} system there is an ultraviolet absorption peak centered at 273 nm. These spectra are discussed in Chapter V.

Treatment of Samples with Water Vapor

A sample each of KCl:Pb^{2+} and KCl:Cd^{2+} was treated with water vapor in order to determine the effect of this treatment on the polarization observed. The results of these experiments are discussed in Chapter V.

Each sample was placed in a separate Vycor tube. The tube in turn was connected to the vacuum line and evacuated. A tube containing a small quantity of water was also connected to the vacuum system and pumped on until the water boiled and the volume was reduced to about one half. The vacuum system, the individual sample tube and the tube containing water were joined with a three way stopcock. This allowed the sample tube and the tube containing water to be independently evacuated. After this was done, the two tubes were connected so that the sample tube was filled with water vapor at room temperature. The vapor pressure of water at 24°C is 22.4 mm over liquid water. The Vycor sample tube was sealed and heated in a furnace for 1 1/2 hours at 400°C. Then the sample tube was quenched with liquid nitrogen and allowed to equilibrate to room temperature before opening. After this treatment the sample was plated and vacuum quenched, as described earlier, and polarization measurements were made in the usual way.

V. RESULTS AND DISCUSSION

Data Reduction

Switching Transients

With the circuit described in Chapter IV, when a DCM curve is run there occurs an initial sharp current spike induced due to the switching of the electrometer input. This switching spike will be called induction spike. This spike was usually negative in sign and was short enough in duration to have little effect on the measured current after 10 seconds. But short time currents had to be adjusted for this induction spike. During the time each series of curves was being run, several curves were run at zero potential. The average of these curves, which showed the average contribution of the induction spike, was used to adjust the other curves in the series. The induction correction varied little from series to series, but an average was determined separately for each series so that any change in the induction characteristics between series would not cause over or under correction on the later series.

Separation of Head and Tail Portions of Polarization Curves

Figure 12 shows a typical current vs. time curve on a semi-log plot. Note the linear tail portion and the slightly curved head portion.

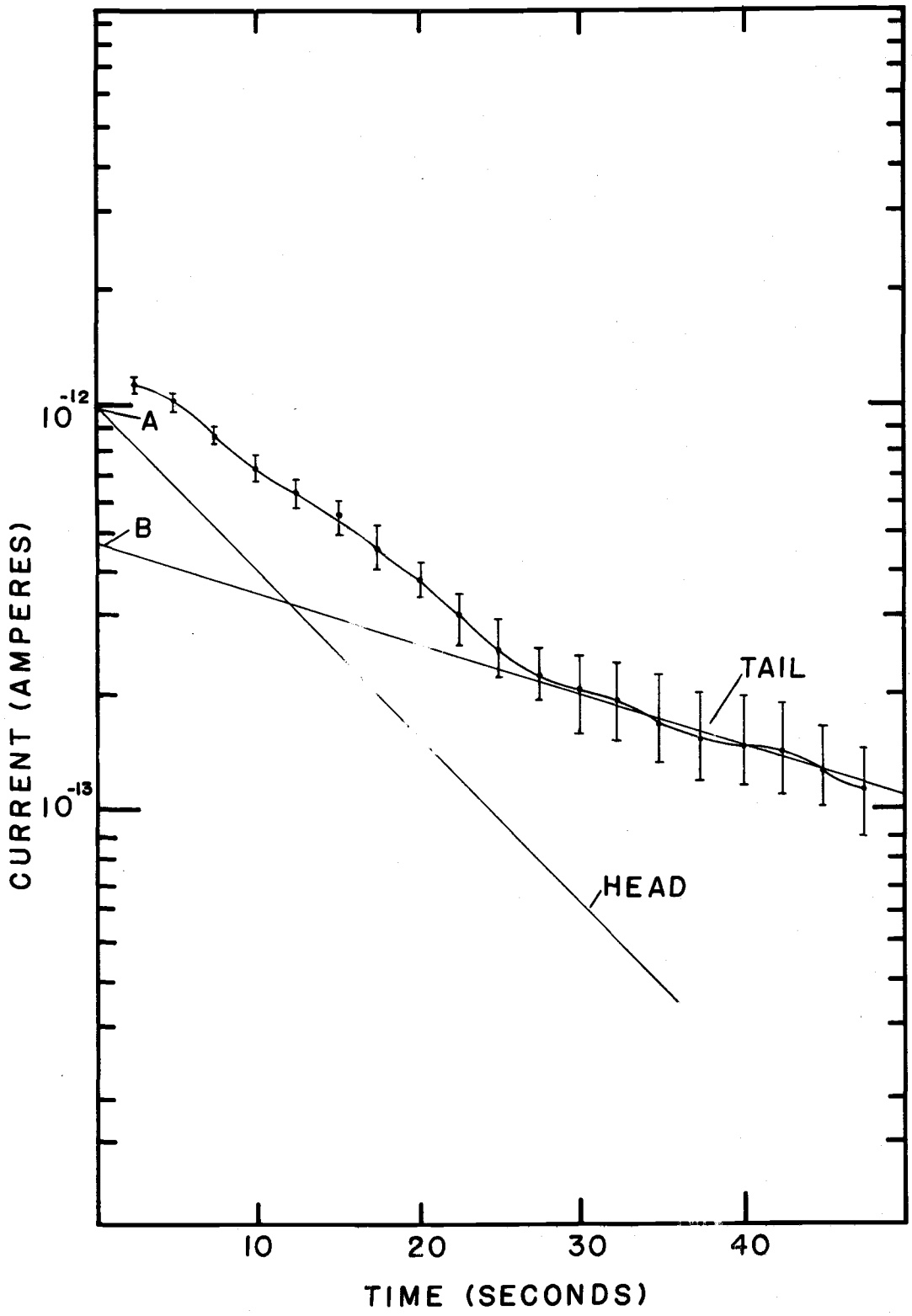

Figure 12. Typical time dependent current curve showing the head and tail portions. This curve is from Series 43 No. 60.

By least-squares fitting the points in the tail of the curve to an exponential function of the form $i = B \exp(-t/\tau)$ a line can be extrapolated to $t = 0$. The difference between this line and the measured curve is the head portion which can be fitted to a similar function. This method can be used if the curve is of the form of Equation (3.19). The constant B is the intercept of the tail portion and A is the intercept determined from the least squares fit of the difference curve (head). The slope of the lines are τ_{Head}^{-1} and τ_{Tail}^{-1} respectively.

This technique is an extension of the method which was used by Dreyfus (1961) and recently was used by Kao et al. (1970) to separate the relaxations they observed. This technique will apply only when the time dependent current observed is the sum of currents contributed by separate sources which have sufficiently different time constants and pre-exponential factors A and B. For most cases in this work, separation was performed with $\tau_2 \geq \sim 3\tau_1$ and $0.1 < B/A < 1$. The required ratio of τ_i values varies with the conditions of the experiment. Examples of this variation are discussed and tabulated in Appendix I.

Experimental Curves

The curves which were obtained by the DCM obeyed Equation (3.19), as predicted. They were exponential curves which varied with

time in the simplest manner for most samples. At low temperatures (less than -50° C) there was no difference between traces taken with either 300 v or 0.00 v applied to the samples. It was concluded that the current recorded in these cases was due only to system transients or inductions as discussed in the first section of this chapter. As the temperature slowly increased the appearance of a slowly decaying current was observed. The shape of these time dependent current curves changed gradually with successive temperature increases, becoming steeper, until the recorded curve was a sharp spike which fell rapidly to zero as the temperature was increased. This behavior was observed for both the KCl:Pb^{2+} and KCl:Cd^{2+} systems.

Long Term Relaxations at Higher Temperatures

In some cases there remained a slowly decaying polarization current at the high end of the temperature range considered. It was small in magnitude and difficult to resolve. It was similar to the "slow" polarization described by Dreyfus (1961) in NaCl systems, which he attributed to IV dipoles with bond length greater than 2 a. Kao et al. (1970) studied short term relaxations for KCl in the region from 100 to 300°C. They used a pulse dc technique and concluded that the process observed was due neither to an IV dipole nor a space charge (electrode blocking) mechanism, but instead a mechanism involving the dislocations within the crystal. This was also observed

in pure and doped NaCl systems. Since most of the impurity ion content in the samples could be accounted for by nn IV dipoles, as discussed later, it is probable that the residual relaxations with high time constant values which were observed near 260°C are due to centers which are related to the dislocation mechanism described by Kao et al. They were not observed in all series of curves which suggests either that the samples were well compensated for by the pure reference crystal, that the pure sample contained fewer dislocations than the doped sample due to slight differences in thermal history or that the positive ion vacancy contribution of the impurity to the Schottky product discussed in Chapter II enters into the dislocation mechanism.

Dipole Effects

Activation Energy

The time constants (τ) obtained from the experimental curves are related to the activation energy (ϵ) for the dipole reorientation process as described in Chapter II by

$$\tau^{-1} = A \exp -\epsilon/kT \qquad (5.1)$$

where A is the frequency factor, k is Boltzman's constant and T is the absolute temperature. Plotting $\ln \tau$ vs $1/T(°K)$ then gives

$+\epsilon/k$ as the slope of the line.

Figures 13 and 14 show the least squares fit of the data obtained from the DCM measurements made on the KCl:Pb^{2+} and KCl:Cd^{2+} samples respectively which were used for this work. The curves are a composite of all the series which were run except those in which the crystals were exposed to water vapor as described later. In some cases where points were taken at the same temperature or within ±0.5°K they were averaged and are indicated by the symbols in the figures. The points themselves are also included. In the least squares fitting process these average points were weighted according to the number of points used in the average.

The figures include four different series for lead and three for cadmium. The activation energies obtained from the slopes are 0.691 ± .01 ev for lead and 0.636 ± .01 ev for cadmium. Table 1 lists the values obtained by various methods for these and other systems. Also listed are the values of A. The curve fitting data for the individual curves are listed in Appendix II.

The activation energies obtained for this work agree quite well with the energies obtained from other methods. However, there is a major difference between the results for KCl:Pb^{2+} shown in Figure 13 and that reported in the literature. The relaxation process in the KCl:Pb^{2+} system was observed in a temperature range about 15°K higher than expected based on the work of Dreyfus (1961) with other

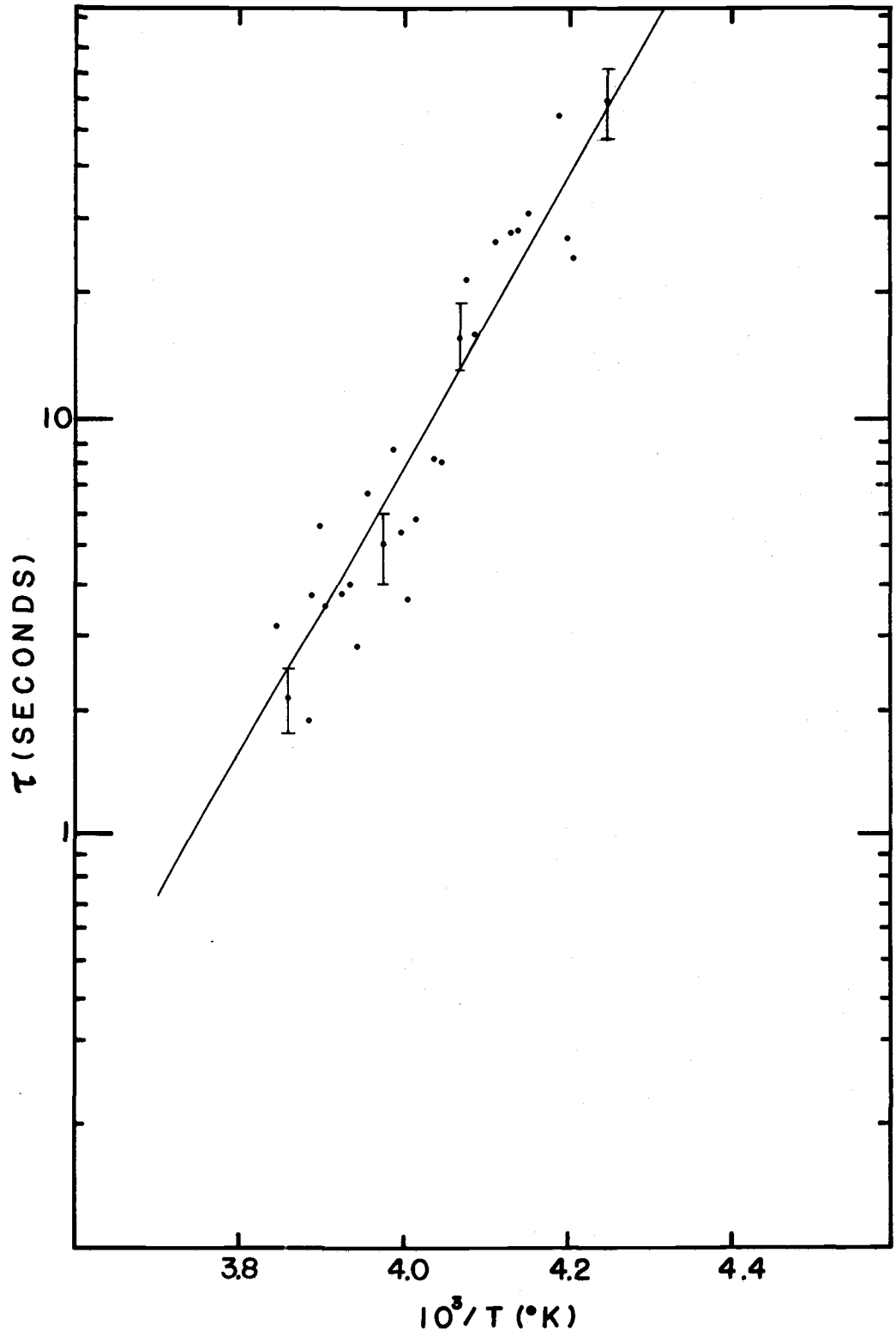

Figure 13. Results for KCl:Pb^{2+} from DCM measurements. All points have similar error limits. Only a few limits are shown for clarity.

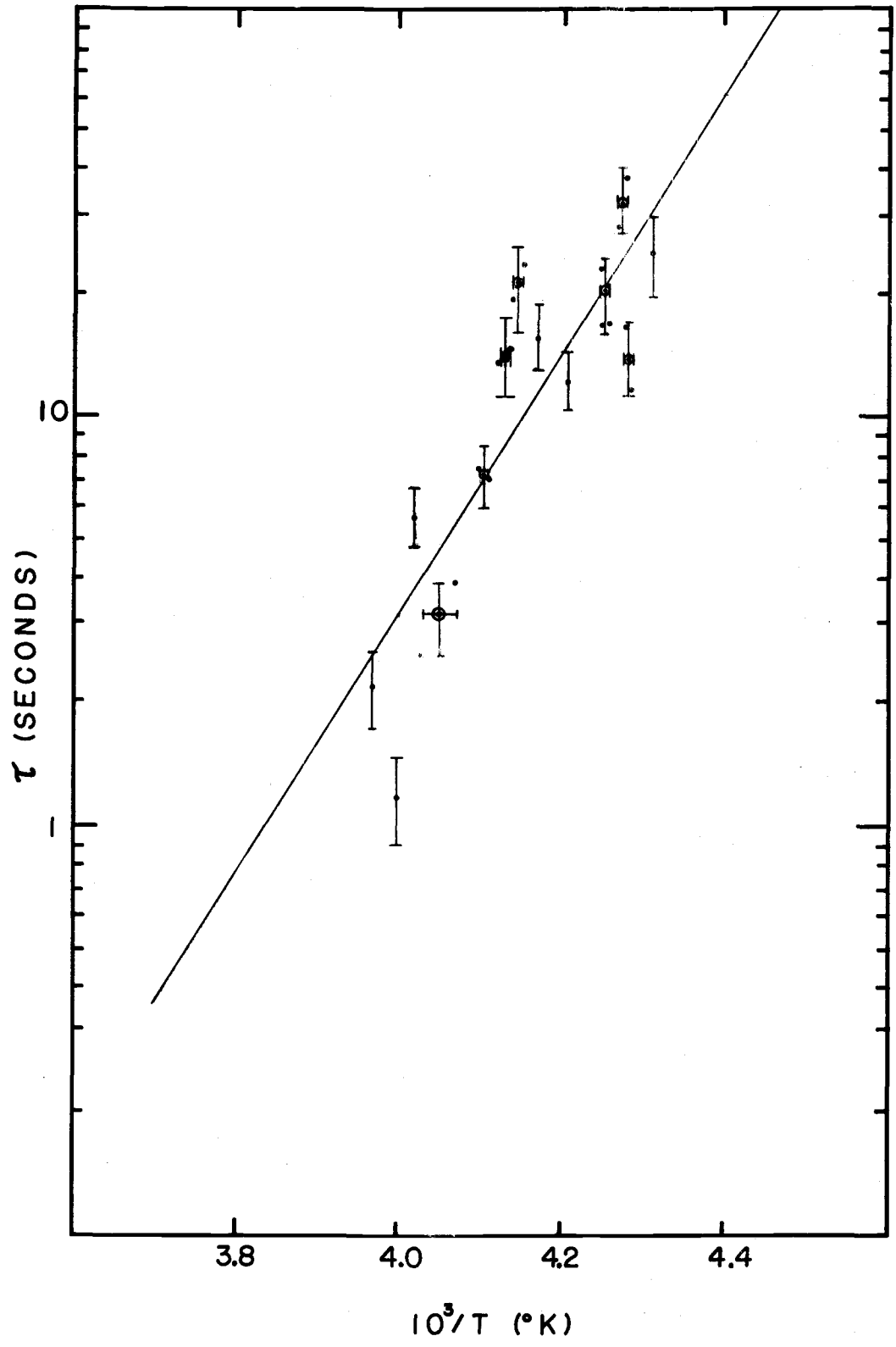

Figure 14. Results for KCl:Cd^{2+} from DCM measurements. Symbols indicate average of data points which are shown.

Table 1. Tabulation of DCM and literature values of activation energy and frequency factor for dipole reorientation in KCl.

M^{2+} Ionic Radius (A)	ϵ (ev)	A (sec^{-1})	Source
Ba^{2+}	0.71 ± .01	3.1×10^{13}	Brun et al. (1970)
(1.37)	0.70	1.3×10^{12}	Dryden and Meakins (1957)
	0.70	2.5×10^{13}	Cook and Dryden (1962)
Sr^{2+}	0.63 ± .01	2.7×10^{12}	Brun et al. (1970)
(1.15)	0.67	1.3×10^{12}	Dryden and Meakins (1957)
	0.67	2.5×10^{13}	Cook and Dryden (1962)
	0.657	9.1×10^{12}	Bucci et al. (1966)
	0.66		Meakins, Progress in Dielectrics (as cited by Suptitz and Teltow, 1967)
Ca^{2+}	0.61 ± .01	3.3×10^{12}	Brun et al. (1970)
(0.99)	0.64	1.3×10^{12}	Dryden and Meakins (1957)
	0.63	2×10^{13}	Bucci et al. (1966)
Pb^{2+}	0.65 ± .01	4.8×10^{12}	Brun et al. (1970)
(1.27)	0.691 ± .01	1.19×10^{13}	This work
Cd^{2+}	0.636 ± .01	2.06×10^{12}	This work
(0.96)			

dopants in NaCl systems and the results from ITC measurements for $KCl:Pb^{2+}$. Cappelletti and Fieschi (1969) while studying the aggregation of IV dipoles in alkali halides observed that the maximum in the ITC curves for $KCl:Pb^{2+}$ occurred as a T_m of 220°K. Brun et al. (1970) found the peak at 223.5°K, also using the ITC method. The relationship between T_m and ϵ is given by

$$kT_m^2 = b\epsilon[\tau(T_m)] = b\epsilon\tau_o \exp(\epsilon/kT_m) \qquad (5.2)$$

where b is the warming rate, ϵ is the activation energy, $\tau(T_m)$ is the time constant at T_m and k is the Boltzman constant. Using Equation (5.2) the time constant at 223.5°K can be calculated using the data reported by Brun et al.;

$$\tau(T_m) = kT_m^2/\epsilon b = 66.2 \text{ seconds} \qquad (5.3)$$

where k is 8.62×10^{-5} ev/°K, b is 0.1°K/sec, ϵ is 0.65 ev and T_m is 223.5°K. This value for τ corresponds to a temperature 15°K lower than predicted from the results of the DCM (see Figure 14). An explanation of this anomaly is discussed in the next section.

Effect of Water Vapor on Polarization of KCl:Pb^{2+} and KCl:Cd^{2+} Samples

In both of the ITC reports cited in the previous section, the salt used for sample preparation was not treated with HCl or Cl_2. Burton and Dryden (1970), in studying the aggregation of IV dipoles noted that in KCl:Pb^{2+} (also without HCl or Cl_2 sample treatment), a broader dielectric absorption band was found than expected. This broadening was attributed to the presence of more than one type of dipole.

Fritz et al. (1963) and Allen (1968) have shown that divalent metal ions interact strongly with hydroxide ions. Therefore; an experiment was conducted to determine the effect of water vapor on the polarization properties of the KCl:Pb^{2+} and KCl:Cd^{2+} systems. The experiment is described in Chapter IV. A sample of each system was tested. The results will be discussed separately.

The KCl:Cd^{2+} sample which was treated with water vapor gave no observable polarization current after the water vapor treatment described in Chapter IV. Crystals which were not treated with water vapor exhibited polarization currents. For this sample, apparently the quenching conditions were not adequate and the interaction between the cadmium and hydroxide ions was too strong for the observation of polarization phenomena in this temperature range.

One of the KCl:Cd^{2+} samples which had been exposed to the

atmosphere at room temperature for nearly one year was measured using the DCM. It was vacuum quenched after plating. As in the case of the previously mentioned KCl:Cd^{2+} sample, no polarization current was observed. This sample was again vacuum quenched, this time after 10 minutes at 450°C. Figure 15 shows the τ vs $10^3/T$ plot from the resulting curves. These values fall into two groups. Curve B is the best least squares fit for the τ values in the range of 217 to 227°K. Curve A is the least squares from the DCM for KCl:Cd^{2+} from Figure 14. There were no τ values observed between the two curves.

These sets of points give a clear indication that two relaxation processes are occurring with a transition between the dominant process under these experimental conditions observed in the region of 225°K.

Figure 16 shows a plot of τ vs $10^3/T$ for the KCl:Pb^{2+} sample which was treated with water vapor. The solid line A is the least squares fitted curve for DCM measurements on KCl:Pb^{2+} as shown in Figure 13. Line B is based on the ITC work of Brun et al. It was plotted using Equation (5.1) and the reported values of τ_o and ϵ (see Table 1). τ values were calculated at various temperatures and line B was drawn through them. The best fit of the experimental points gives: $r = -0.857$, $A = 1.59 \times 10^{-6}$ and $\epsilon = 0.33$ ev. However the group of points at low temperature cluster

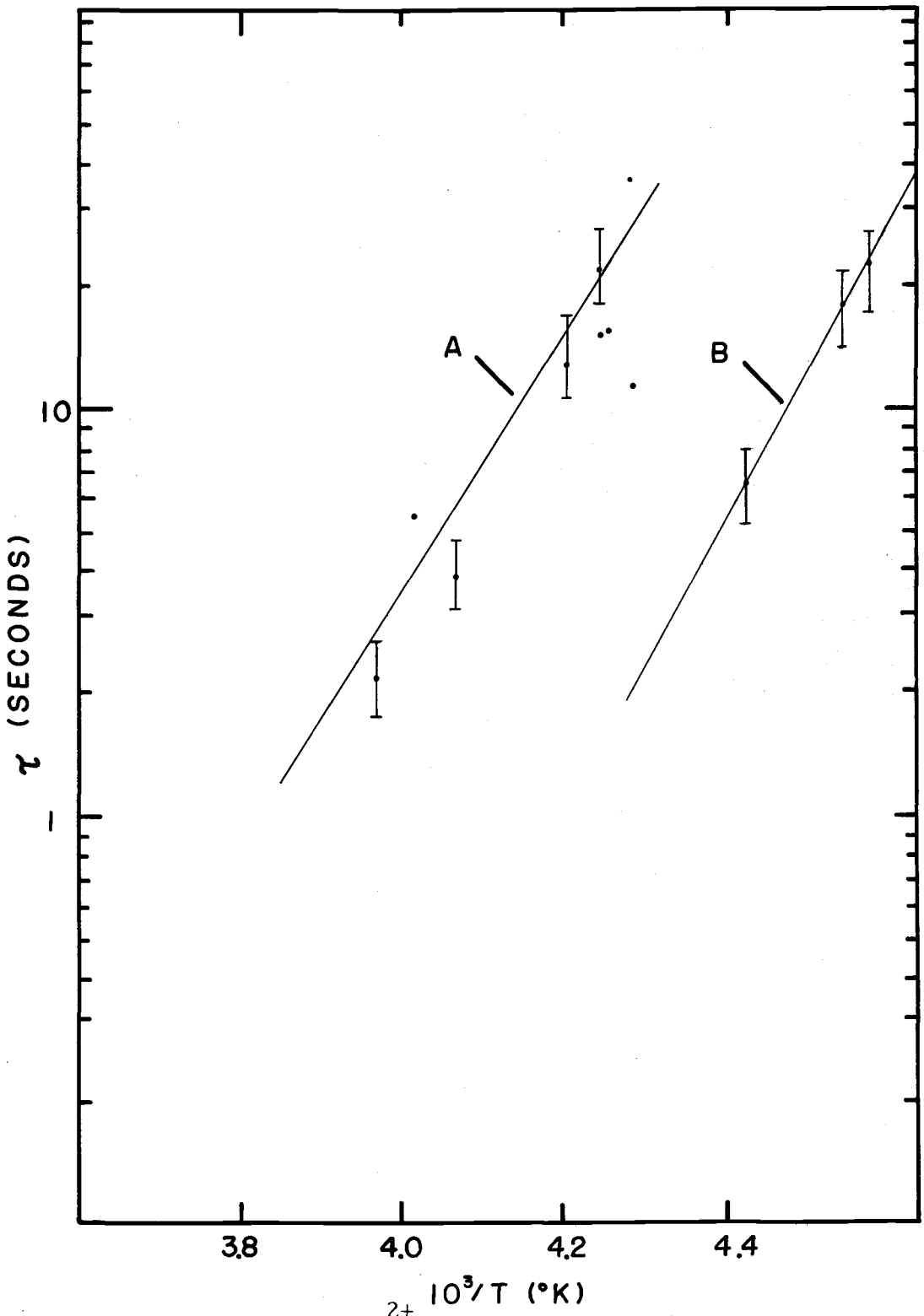

Figure 15. Results for KCl:Cd^{2+} (atmospheric H_2O) experiment:
A) least squares fit for KCl:Cd^{2+} from Figure 14,
B) curve fitted to low temperature points, $\epsilon = 0.61$ ev,
$A = 1.90 \times 10^{-13}$ and $r = -0.999$.

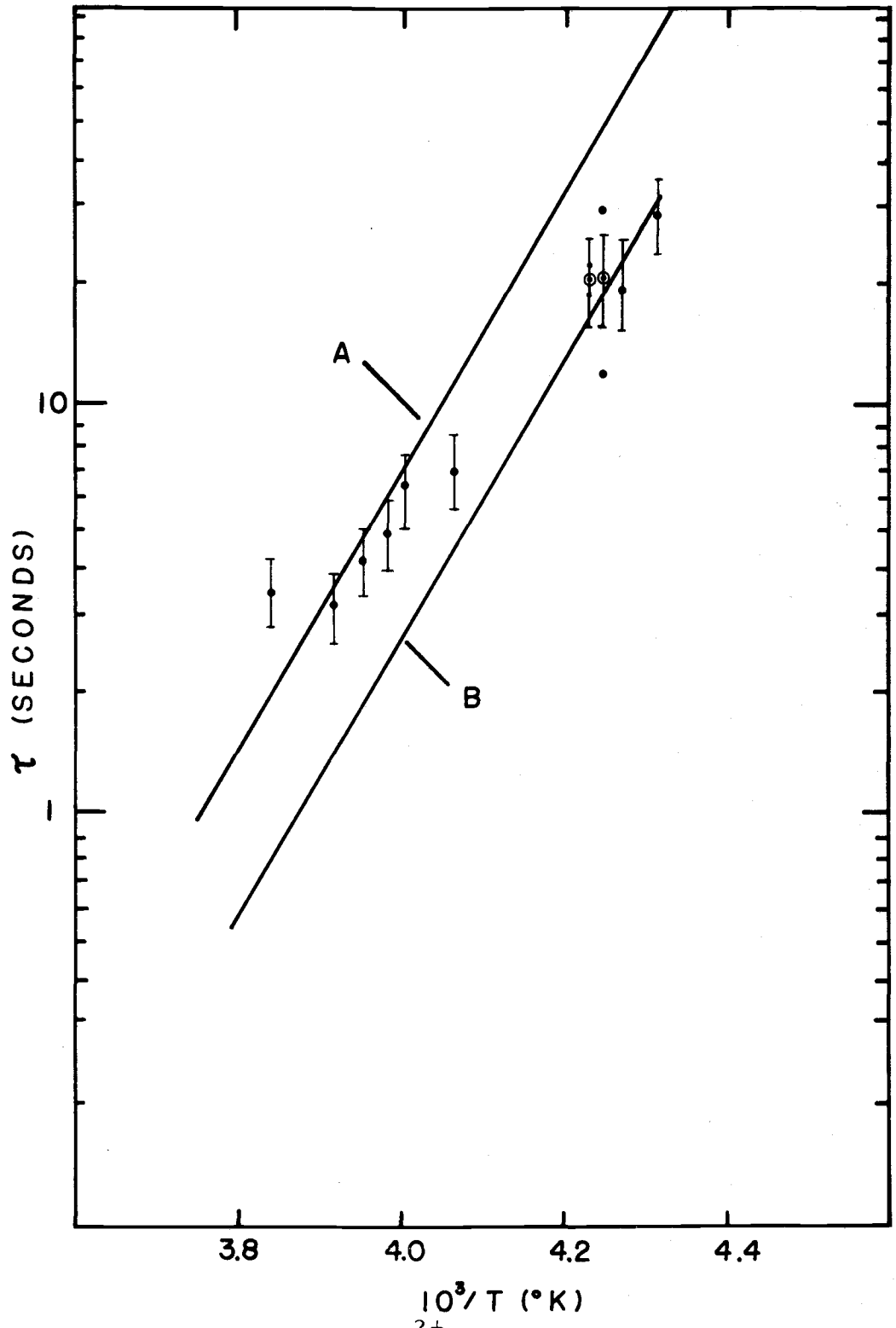

Figure 16. Results for KCl:Pb^{2+}-H_2O experiment: A) DCM result from Figure 13, B) calculated from data of Brun et al. and Equation (5.1). Symbols indicate average of data points shown.

around the curve calculated from Brun et al. and give: $r = -.993$, $\epsilon = 0.35$ ev and $A = 5.82 \times 10^{-7}$. The higher temperature data which fall near the DCM curve give: $r = -.986$, $\epsilon = -0.56$ ev and $A = 3.46 \times 10^{-11}$. While there are insufficient data to precisely determine whether the observed relaxation is due to a single species or two distinct processes as shown for KCl:Cd^{2+}, the curve fitting data indicate that the latter is more probable.

The results for the two KCl:Cd^{2+} samples lead to the conclusion that the interaction of the cadmium doped samples with hydroxide is a strong and rapid one which is difficult to observe under the conditions used in this work. The interaction of the sample with atmospheric water vapor at room temperature takes a much longer time than the interaction with water vapor at 400°C due to the reduced rate of diffusion of hydroxide ions at the lower temperature (refer to Allen and Fredericks, 1970).

In both of the cases just described the relaxation process observed was altered when a crystal sample was put in contact with water vapor. The change in polarization can be ascribed to the interaction of the IV dipoles with OH^-. While the evidence for the KCl:Pb^{2+} system is not conclusive, taken with the work of Brun et al. and Burton and Dryden it shows that the different observations for the system by the ITC and DCM techniques are probably due to the different methods used in crystal growth and sample preparation. This emphasizes the importance of excluding OH^- from crystals used in the study of polarization processes.

Concentration of Dipoles and Efficiency of Quenching

Heating of the crystals containing aggregates of IV dipoles will cause the aggregation process to reverse and increase the number of dipoles present in the crystal as described by Cook and Dryden (1962) and Dryden and Harvey (1969). Table 2 shows the concentration of impurity ions determined by polarography and the concentration of dipoles which contributed to the DCM polarization as calculated by Equation (2.9). Also involved in fixing the dipole concentration is the process of dissociation of the IV dipoles into free vacancies and cations as described in Chapter II. The degree of association (p) at 400°C is listed for each concentration based on the concentration determined by polarographic analysis.

Table 2. Concentration of impurity ions and dipoles.

Series	Doped Sample	Concentrations: Dipoles (DCM) mf x 10^6	Concentrations: Ions (polarography) mf x 10^6	Dipoles / Ions	p (at 400°C)
43	Pb1	62.8 ± 12*	55.0 ± 5	1.14	.56
44	Pb1	26.7 ± 6	55.0 ± 5	.48	.56
47	Pb3	38.3 ± 8	57.0 ± 5	.67	.58
48	Pb2	35.2 ± 7	70.0 ± 7	.50	.71
49	Cd1	8.7 ± 8	59.3 ± 6	.15	.59
52	Cd2	21.4 ± 5	45.8 ± 5	.47	.46
56	Cd3	17.8 ± 4	80.1 ± 8	.22	.80

*This error was determined by propagation of error techniques and does not include the systematic error from zero current line placement.

The series numbered 43 and 44 were run using the same $KCl:Pb^{2+}$ sample (Pb-1), but with a different reference crystal. Pb-1 was quenched and plated prior to Series 43. Series 44 was taken four days later without further quenching operations. The concentration of dipoles was reduced during this time indicating that the aggregation process takes place fast enough at room temperature to require that the study of dipolar behavior at low temperatures should be directly preceded by quenching in order to insure a maximum dipole concentration as concluded by Dryden and coworkers. The high value for the ratio of concentration of dipoles to the concentration of divalent impurities for series 43 seems unlikely. It is probable that this is due to a systematic error in the placement of the zero line and resulting value of j_o used in Equation (2.9) for the calculation.

The quenching temperature which insures the maximum concentration of dipoles varies with the impurity ion which is incorporated in the lattice as shown by the difference in the percentage of dipoles present in the two systems investigated. The difference observed for the two systems can result from two causes. Either the quenching temperature was not high enough to sufficiently reverse the IV dipole aggregation for the $KCl:Cd^{2+}$ samples or the reformation rate of these clusters was so rapid that the quenching rate was not fast enough to freeze them all into the lattice.

The percentage of dipoles could be increased with respect to the

total divalent cation concentration by experimentally determining the optimum quenching conditions for each system. However; it is apparent that for the purpose of this work 400°C is a sufficiently high temperature and the vacuum quenching technique is sufficiently rapid to obtain a dipole concentration large enough to observe the polarization effects.

Correlation of Impurity Radius with Activation Energy

According to the Dreyfus theory outlined in Chapter II, the activation energy for dipole realignment should change as the radius of the impurity ion changes. Figure 17 shows the values obtained by the DCM for KCl as well as activation energies for other ions described in the literature. The apparent trend is for the activation energy to decrease as predicted and shown to be the case for NaCl systems by Dreyfus (1961). Several different methods were used including dielectric loss, ITC and DCM.

For impurity cations with ionic radii slightly smaller than that of the host lattice cation, a transition takes place between the two limiting cases which describe the favored configuration. Briefly, in Case II the nn IV dipole configuration is favored and the observed relaxation is contributed by the nn form. This is the case when the impurity ion radius is the same or larger than the host cation. In Case I the nnn configurations contributes the major portion of the

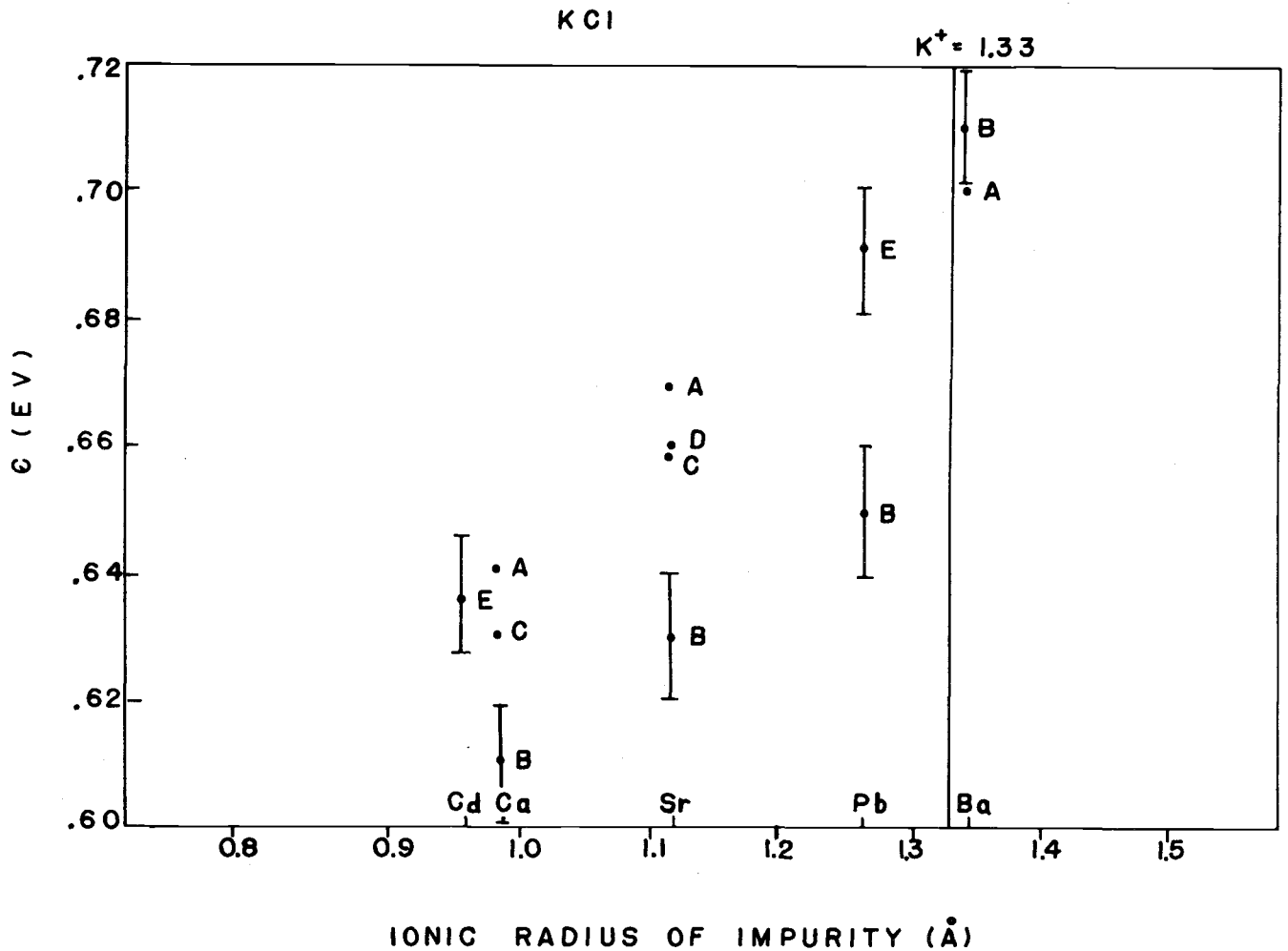

Figure 17. Relationship between ϵ and impurity radius: A) Dryden and Meakins (dielectric loss), B) Brun et al. (ITC), C) Bucci (ITC), D) Meakins (dielectric loss), E) DCM.

polarization observed. This case is favored when the impurity cation is about 15% smaller than that of the host cation. It can be seen from the illustration that the activation energy does gradually decrease with impurity radius in the range from 1.4 to 0.9 Å. This does support the Dreyfus theory.

Brun et al. have questioned the validity of the theory because of the work of Bucci (1967) with the KCl:Be^{2+} system. Bucci concluded that the vacancy could be in the nn position as well as the nnn position predicted by the theory. Be^{2+} is a very small ion with an ionic radius of 0.38 Å. This extremely small size effects the relaxation properties of crystal in a unique manner. The exchange of the impurity with the vacancy is the factor which determines the relaxation rate, i.e., the exchange frequency (ω_2) is greater than the others. Also Be^{2+} ion may not be centered in a K^+ ion site as the larger impurity ions are. The off center position would also effect the application of the theory. Thus the behavior of the KCl:Be^{2+} system would be difficult to predict and is perhaps beyond the radius limits in which the theory would apply. The study of ions in the radius range between 0.70 and 0.9 Å such as Zn^{2+} (0.72 Å) Mn^{2+} (0.78 Å) and Ni^{2+} (0.73 Å) would help to resolve this question.

Effect of Plating Procedure and Sample Selection

The electrodes produced by vacuum plating gold on freshly

cleaved crystal surfaces can contribute spurious signals to electrical measurements as shown by Seevers and Scott (1970). When pure crystal samples cleaved from the same boule, with the same thickness and same plating treatment were placed in the DCM apparatus the resulting traces indicated definite differences in the properties of electrodes as shown in Figure 18.

Sanding of the crystal surface improves the ohmic nature of the contacts, but this process introduces many more locations for air gaps to be formed when the gold is deposited. It was found that when sanded pure crystals were used as the DCM standard no usable relaxation curves were obtained. A large relaxation current was present which was independent of temperature and which was not present when unsanded, quenched crystals were put in place of the sanded samples. Series 47 was run with a doped crystal (Pb3) which had been plated without sanding and was not quenched. The reference sample (P7) was lightly sanded before plating. The first several curves indicated that there was a large mismatch in the samples or a failure in the electrical connections. The circuit was modified slightly by disconnecting the power supply from the pure sample and measurements were made by only applying the electric field to the doped sample. The resulting curves for low temperature showed a nearly constant decay current while as the temperature was raised, this current increased in magnitude as expected. The data listed in Appendix II

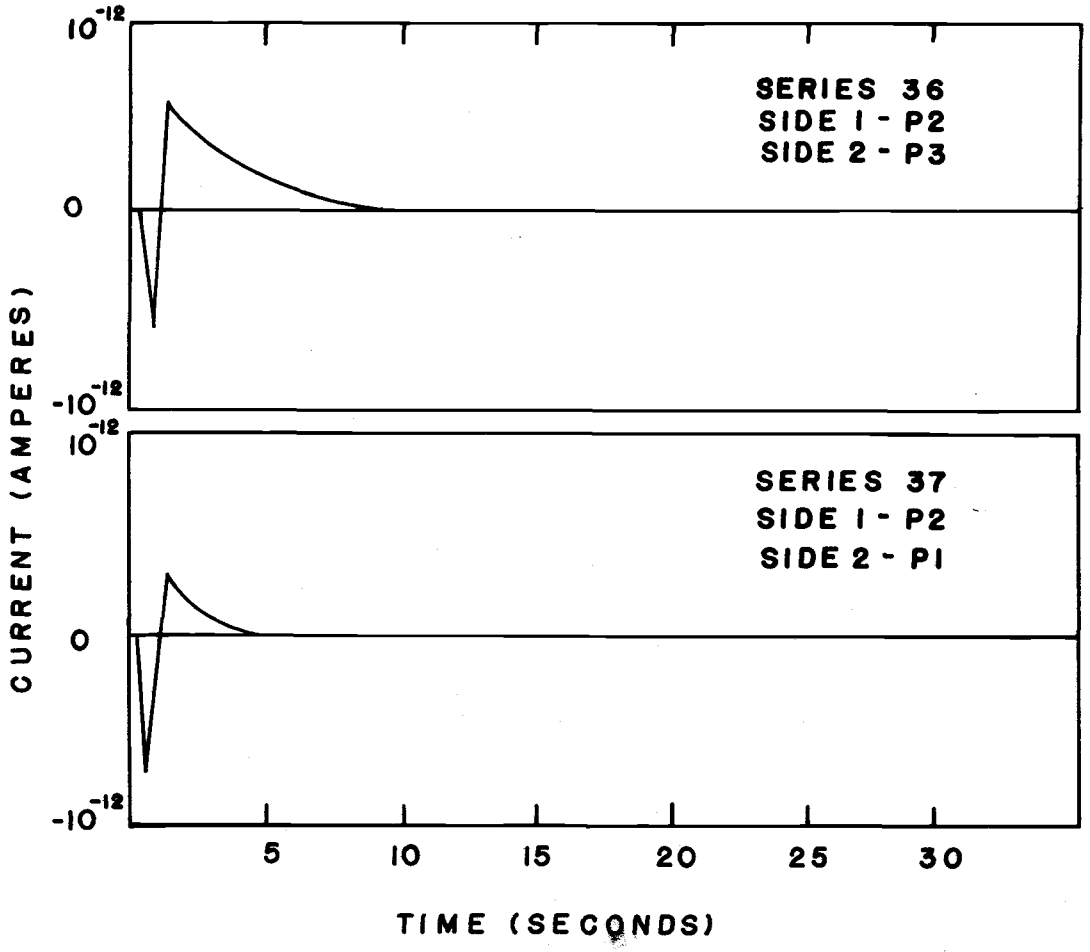

Figure 18. Difference in observed polarization current due to plating for freshly cleaved pure samples: $V_1 = -V_2 = 150$ v, temperature is 24°C.

for Series 47 have been adjusted by averaging the low temperature curves and subtracting that average point by point from the experimental curves at higher temperatures. The change in τ with increasing temperature for this series is the same as for the other KCl:Pb^{2+} series shown in Figure 13. This series illustrates that the sanding of samples surfaces greatly affects polarization measurements. When compared with other series it shows that the DCM, when used with properly matched crystals, is effective in reducing residual polarization effects by matching opposing branches of the circuit and in this way isolates the polarization effects due to differences in the crystals themselves and the power branches of the circuit.

When the freshly cleaved plated samples were vacuum quenched to room temperature they gave no detectable relaxation contribution which could be attributed to other than dipolar effects. The DCM curves for doped vs pure crystals which were quenched after plating showed only an induction spike at low temperatures. As the temperature was raised the temperature dependent polarization of the dipoles became evident.

Usually the plated samples were heated for 8 minutes for the vacuum quenching process as described in Chapter IV. When a plated sample was heated for an hour, the gold diffused into the sample and sublimed from the surface to such an extent that the resistance of each

surface as measured with two point probes of a VOM was greater than 10^6 ohms. As the test probes were moved closer together, no difference in the reading was observed even though the crystal appeared to still have shiny gold plated surfaces.

It was concluded that the vacuum quenching procedure improves the characteristics of the electrode-crystal junction by allowing gold from the electrode to diffuse a short distance into the sample.

After the perfection of the plating with vacuum quenching technique there were no polarization effects observed in this work such as described in Chapter III due to either crystal thickness mismatch or electrode contributions.

The first effect was reduced by choosing doped and reference samples which were within ±2% of each other in thickness. Most of the DCM measurements were made by using the 10^{10} ohm shunt resistor in the electrometer. For these reasons the mismatch polarization (shown in Figure 3 for a 9.4% mismatch) was not observed.

Electrode contributions to the polarization appeared to be reduced by vacuum quenching technique so much that they were not large enough in magnitude to be observed or these contributions were efficiently compensated by the reference sample of the DCM.

UV Absorption Specta of the KCl:Pb^{2+} and Pure Samples

The pure crystals used in this work showed a flat uv absorption spectrum which is characteristic of KCl. There were no bands which could be attributed to OH^- (204 nm) or other oxygen containing species.

The samples of KCl doped with Pb^{2+} exhibited only the strong absorption band at 273 nm which is characteristic of $PbCl_2$ (DeVries and Van Santen, 1964) and Pb^{2+} in KCl (Sibley et al., 1964 and Holmes, 1966). Holmes, Burstein et al. (1951) among others observed side bands for the 273 nm absorption. These bands have been assigned to lead interactions with other lead ions in aggregates and with oxygen containing species. Dryden and Harvey (1969) assigned some of these side bands to the interaction of IV dipoles during the aggregation process. The lead doped samples used in this work exhibited none of these side bands. The absence of a peak in the region of 260 nm, which has been assigned to the interaction of Pb^{2+} with oxygen containing species, indicates the absence of large amounts of hydroxide ion. The absence of the 290 nm band assigned to the Pb-Pb interaction and other aggregation bands taken with a fairly high percentage of dipoles available as shown in Table 2 indicates the absence of appreciable aggregation in the samples. It should be noted that the spectra of the KCl:Pb^{2+} samples were taken immediately after quenching, therefore; the aggregation bands (cited by Dryden and Harvey, 1969)

which grew with time at room temperature would not be expected to appear. The lead doped sample which was treated with H_2O vapor showed a slight decrease in absorbance.

Cadmium doped KCl samples have no absorption peaks in the uv. There is an absorption band outside the short wave length edge of the region which has a shoulder which carries over into the uv. The spectra of KCl:Cd^{2+} samples used in this work were taken only to indicate the presence of this shoulder. No other uv absorptions were observed in any of the samples used.

Summary

The DCM was developed to provide a self correcting method of observing the IV dipolar properties of KCl doped with Pb^{2+} and Cd^{2+}.

It was found that for the KCl:Pb^{2+} system, the observed polarization occurred in a higher temperature range than expected based on reported findings from the ITC technique. When a sample of KCl:Pb^{2+} was heated in the presence of water vapor, a change in the polarization process was observed. There were τ values observed which agreed with both the ITC and DCM results, however the data was not separable into two distinct relaxation processes.

A KCl:Cd^{2+} sample showed no polarization when treated with water vapor. A KCl:Cd^{2+} sample which had been exposed to atmospheric water for an extended period of time however exhibited a low

temperature polarization as well as one in a higher temperature range which was the same as other DCM samples. It was concluded that the polarization observed in the lower temperature range was due to the interaction of the IV dipoles with OH^- and that the pretreatment of the KCl with HCl and Cl_2 before sample growth would eliminate the problem.

The change in activation energy for IV dipole reorientation was found to support the Dreyfus theory.

Proper electrode preparation is critical to the correct measurement of polarization properties. It was found that vacuum quenching samples after the vapor deposition of gold on the surface decreased the spurious relaxation current from the electrodes. Matching of crystal thickness (within ±2%) resulted in the elimination of observable current due to sample thickness mismatch.

Vacuum quenching of the samples before plating resulted in a dipole concentration within the expected range. This process was more efficient for lead than cadmium doped samples.

BIBLIOGRAPHY

Allen, C. A. 1969. Diffusion, conductivity and spectral properties of mercury II ion in potassium chloride crystals. Ph. D. thesis. Corvallis, Oregon State University. 141 numb. leaves.

Allen, C. A. and W. J. Fredericks. 1970. Diffusion of hydroxide ion in potassium chloride single crystals. The Journal of Solid State Chemistry 1:205-209.

Allnatt, A. R. and P. W. M. Jacobs. 1961. AC polarization effects in the ionic conductivity of potassium chloride. Journal of the Physics and Chemistry of Solids 19:281-290.

Beaumont, J. H. and P. W. M. Jacobs. 1967. Polarization in potassium chloride crystals. Journal of the Physics and Chemistry of Solids 28:657.

Breckenridge, R. G. 1948. Low frequency dispersion in inoic crystals. Journal of Chemical Physics 16:959-967.

Breckenridge, R. G. 1950. Low frequency dispersion in ionic crystals containing foreign ions. Journal of Chemical Physics 18:913-926.

Brun, A., P. Dansas and P. Sixon. 1970. Study of the reorientation of I. V. complexes in KCl containing divalent substitutional ions. Solid State Communications 8:616-613.

Bucci, Cesare. 1967. Ionic thermalcurrents in alkali halide crystals containing Be^{2+}. The Physical Review 164:1200-1206.

Bucci, C., R. Cappelletti, R. Fieschi, G. Guidi and L. Pirola. 1966. Ionic thermalcurrents in dielectric solids. Il Nuovo Cimento, Supp. 4:607-629.

Bucci, C., R. Fieschi and G. Guidi. 1966. Ionic thermalcurrent in dielectrics. The Physical Review 148:816-123.

Bucci, C. A. and S. C. Riva. 1965. Evidence for space charge polarization in pure KCl at low temperatures. Journal of the Physics and Chemistry of Solids 26:363-371.

Burstein, E., J. J. Oberly, B. W. Henvis and J. W. Davisson. 1951. A note on the distribution of impurities in alkali halides. The Physical Review 81:459-460.

Burton, C. H. and J. S. Dryden. 1970. The intensity of the dielectric absorption in alkali halides containing divalent cations. The Journal of Physics. C. Solid State Physics 3:523-530.

Cappelletti, R. 1968. Colour centers induced by cadmium addition in sodium chloride. Il Nuovo Cimento. LIV B:233-244.

Cappelletti, Rosanna and Edmondo DeBenedetti. 1968. Aggregation of divalent impurities in sodium chloride doped with cadmium. The Physical Review 165:981-985.

Cappelletti, R. and R. Fieschi. 1969. Solubility of metal impurities in alkali halides measured by means of ionic thermalcurrent. Crystal Lattice Defects 1:69-81.

Cook, J. S. and J. S. Dryden. 1960. The intensity of dielectric absorption in alkali halides as a function of the concentration of divalent cation impurities. The Australian Journal of Physics 13:260-269.

Cook, J. S. and J. S. Dryden. 1962. Investigation of the aggregation of bivalent cationic impurities in alkali halides by dielectric absorption. Proceedings of the Physical Society (London) 80:479-488.

Di Giura, V. and G. Spinolo. 1968. Measurement of the low-frequency dielectric constant in some alkali halides. Il Nuovo Cimento 56B:192-4.

De Vries, K. J. and J. H. Van Santen. 1964. Ultraviolet absorptions of non-stoichiometric lead chloride, $PbCl_2$. Physica 30:2051-2058.

Dreyfus, R. W. 1961. Dielectric relaxation due to impurity-vacancy complexes in NaCl crystals. The Physical Review 121:1675-1687.

Dryden, J. S. 1963. The aggregation of bivalent impurities and their associated cation vacancies in alkali halides. Journal of the Physical Society of Japan, Suppl. 18:129-133.

Dryden, J. S. and G. G. Harvey. 1969. Dielectric and optical properties of lead-activated sodium and potassium chloride crystals. Proceedings of the Physical Society, London, Solid State Physics. [2]: 2:603-618.

Fredericks, W. J.. L. W. Schuerman and L. C. Lewis. 1966. An investigation of crystal growth processes. Prepared for Grant No. AF-AFOSR-217-63. Project Task: 9762-02 Solid State Sciences Division, Air Force Office of Scientific Research, Washington, D. C. January. 40 numb. leaves.

Friauf, Robert J. 1954. Polarization effects in the ionic conductivity of silver bromide. Journal of Chemical Physics 22:1329-1338.

Fritz, Bernd, Fritz Luty and Jorg Anger. 1963. Dere Einfluss von OH^- -Ionen auf Absorption spektrum und Ionenleitfahiglseit von KCl - Einkristallen. Zeitschrift fur Physik 174:240-256.

Hattori, Takeshi, Yoshinori Chiba and Hideo Futama. 1967. Sr^{2+}-$(OH)^-$ interaction in KCl crystals. Journal of the Physical Society of Japan 23:137-138.

Haven, Y. 1953. Dielectric loss of sodium chloride crystals. Journal of Chemical Physics 21:171-172.

Holmes, Robert E. 1966. Electrical and optical properties of potassium chloride single crystals containing lead ions. Ph. D. thesis, Corvallis, Oregon State University. 191 numb. leaves.

Jacobs, P. W. M. and J. N. Maycock. 1963. Polarization effects in the ionic conductivity of alkali halide crystals. I AC capacity. Journal of Chemical Physics 39:757-762.

Kao, K. C., W. Whitham and J. H. Calderwood. 1970. Time dependent polarization in alkali halides. Journal of the Physics and Chemistry of Solids 31:1019-1026.

Keneshea, F. J. and W. J. Fredericks. 1963. Diffusion of lead ions in potassium chloride. Journal of Chemical Physics 38:1952-1958.

Keneshea, F. J. and W. J. Fredericks. 1964. Diffusion of lead ions in solid potassium chloride. Journal of Chemical Physics 41:3271-3272.

Keneshea, F. J. and W. J. Fredericks. 1965. The diffusion of cadmium ions in solid potassium chloride. Journal of the Physics and Chemistry of Solids 26:501-508.

Miliotis, Demitrios and Duk. N. Yoon. 1970. Existence of air gaps in specimen-electrode contacts and their effect on dielectric relaxation phenomena in KCl and NaCl. Journal of the Physics and Chemistry of Solids 30:1241-1249.

Patterson, D. A. 1962. Controlled atmosphere Kyropoulos growth of alkali halide single crystals. The Review of Scientific Instruments 33:831-833.

Seevers, Robert Edward. 1968. Electrical conductivity of additively colored potassium chloride crystals. Ph. D. thesis. Corvallis, Oregon State University. 126 numb. leaves.

Seevers, R. E. and A. B. Scott. 1970. Electrical conductivity of additively colored potassium chloride. Journal of the Physics and Chemistry of Solids 31:729-737.

Sibley, W. A., E. Sonder and C. T. Butler. 1964. Effect of lead on the room temperature colorability of KCl. The Physical Review 136A:537-541.

Suptitz, P. and J. Teltow. 1967. Transport of matter in simple ionic crystals (cubic halides). Physica Status Solidi 25:9-56.

Sutter, P. H. and A. S. Nowick. 1963. Ionic conductivity and time-dependent polarization in NaCl crystals. Journal of Applied Physics 34:734-746.

Watkins, G. D. 1959. Motion of Mn^{2+}-cation vacancy pairs in NaCl: Study by electron spin resonance and dielectric loss. The Physical Review 113:91-97.

Zener, C. 1952. Imperfections in nearly perfect crystals. John Wiley and Sons, Inc., New York. p. 289.

APPENDICES

APPENDIX I

A glance at Figure 12 of the text reveals that the angle with which the head and tail portion of the resolved curve intersect is related to the respective line slopes by

$$\beta = \alpha_1 - \alpha_2 = \tan^{-1}(-\frac{1}{\tau_1}) - \tan^{-1}(-\frac{1}{\tau_2})$$

where α_1 and α_2 are the time intercepts of the head and tail portions. The following table lists some sample values for β determined from the relationship for various common values of τ_1 and τ_2. The slopes were taken as positive to simplify calculation

τ_1	τ_2	β	τ_1	τ_2	β
5	10	5.6°	15	20	0.9°
5	20	8.5°	15	25	1.5°
5	30	9.4°	15	30	1.9°
5	40	9.9°	15	35	2.2°
10	15	2.8°	15	40	2.4°
10	25	3.4°	15	45	2.5°
10	35	4.1°	15	60	2.9°
10	45	4.4°			
10	55	4.7°			

From these values it can be seen that the larger the value of τ_1 (smaller $1/\tau_1$), the larger the ratio of τ_2/τ_1 must be for good separation of the lines. For small τ_1 good separation was accomplished with $\tau_2 \geq \sim 2\tau_1$ while at higher values of τ_1 separation could only be made with $\tau_2 \geq 4\tau_1$ or larger.

APPENDIX II

Tabulation of DCM results from least squares curve fitting.

			Tail			Head		
Series	No.	$\frac{10^3}{T(°K)}$	τ (sec)	$A \times 10^{13}$ (amp)	-r	τ (sec)	$A \times 10^{13}$ (amp)	-r
43	19	4.14	16.0	4.97	.977			
	20	4.09	15.0	8.70	.981			
	21	4.00	37.1	4.91	.992	6.54	16.5	.998
	34	4.15	20.3	9.81	.993			
	35	4.14	23.5	8.79	.992			
	36	4.07	22.9	6.06	.987	9.17	8.44	.943
	37	3.97	9.5	14.3	.998			
	57	4.14	44.3	3.61	.996	14.31	5.78	.990
	58	4.11	25.2	3.73	.992	9.10	8.16	.988
	59	4.08	23.6	4.04	.997	11.42	7.65	.992
	60	4.05	35.8	4.60	.997	10.95	9.79	.999
	61	3.98	57.3	1.99	.989	6.05	15.3	.971
	62	3.91	44.8	3.15	.997	6.76	12.9	.984
	63	3.94	57.5	2.24	.992	4.00	32.1	.975
	64	3.90	32.7	4.22	.996	5.59	1.05	.969
	65	3.95	39.3	4.87	.989	4.79	1.47	.990
44	4	4.25	55.9	2.55	.974			
	5	4.19	67.4	2.71	.978			
	6	4.15	42.8	2.18	.977			
	7	4.07	11.9	6.57	.978			
	8	4.40	8.1	5.34	.995			
	9	4.01	3.6	1.35	.994			
	11	3.91	19.2	2.64	.987	3.59	1.29	.986
	12	3.85	28.1	3.63	.991	4.08	4.72	.999
47	58	4.33	41.3	2.04	.947			
	60	4.20	25.5	3.88	.999			
	61	4.11	88.0	1.98	.959	7.68	9.36	.977
	62	4.07	36.4	3.77	.965	7.16	8.99	.976
	63	4.02	49.9	4.77	.990	5.87	11.1	.999
	64	3.98	38.0	4.28	.993	3.31	22.2	.999
	65	3.95	49.5	4.65	.989	3.84	16.4	.996
	66	3.89	50.9	5.60	.991	3.72	10.6	.963
	69	3.82	42.2	10.8	.992			

Series	No.	$\frac{10^3}{T(°K)}$	Tail τ (sec)	Tail $A \times 10^{13}$ (amp)	Tail -r	Head τ (sec)	Head $A \times 10^{13}$ (amp)	Head -r
48	13	4.19	36.7	3.71	.993			
	14	4.13	26.0	3.92	.996			
	15	4.08	20.3	6.03	.994			
	16	4.05	67.7	1.55	.963	4.79	15.5	.929
	17	4.00	48.3	2.31	.991	4.09	16.3	.990
	18	3.98	4.83	1.28	.993			
	19	3.92	33.4	2.64	.970	4.78	6.79	.996
	21	3.86	26.6	2.38	.989	2.04	2.82	.986
	33	4.21	22.8	2.29	.994			
	34	4.14	22.2	3.00	.994			
	39	4.04	19.4	2.07	.986	7.09	6.02	.987
	40	3.99	8.3	8.79	.978			
	41	3.95	18.2	2.47	.998	2.63	22.8	.988
	42	3.92	19.7	1.97	.989	2.69	13.5	.998
	44	3.88	14.7	2.68	.986	1.85	35.3	.998
	45	3.85	16.9	1.86	.997	2.18	17.3	.999
	46	3.85	18.4	2.41	.998	1.61	37.6	.998
49	27	4.17	14.9	.87	.954			
	32	4.03	2.6	6.94	.993			
52	2	4.12	13.4	3.44	.989			
	5	4.15	23.0	1.67	.985			
	6	4.14	19.7	1.96	.994			
	7	4.13	15.0	1.26	.988			
	9	4.10	7.4	3.01	.951			
	11	4.05	36.7	1.19	.980	3.16	3.12	.972
	12	4.00	13.3	3.97	.989	1.19	3.87	.999
	43	4.31	25.1	.57	.972			
	44	4.28	15.9	1.76	.993			
	45	4.27	28.9	1.94	.965			
	48	4.11	7.2	9.89	.986			
54	11	4.36	9.2	2.06	.976			
	12	4.31	27.7	.94	.996			
	14	4.23	21.8	6.50	.995			
	15	4.23	18.8	4.98	.997			
	16	4.24	11.7	2.84	.996			
	18	4.24	29.1	3.01	.990			
	19	4.27	23.8	3.66	.989			
	21	4.06	6.9	16.6	.998			
	22	4.01	6.4	20.8	.998			

Series	No.	$\frac{10^3}{T(°K)}$	Tail τ (sec)	Tail $A \times 10^{13}$ (amp)	Tail -r	Head τ (sec)	Head $A \times 10^{13}$ (amp)	Head -r
	23	3.98	4.9	26.9	.999			
	24	3.94	4.2	28.4	.996			
	25	3.91	3.2	28.7	.992			
	27	3.87	5.9	4.18	.994			
	28	3.84	3.5	11.2	.998			
56	45	4.26	16.3	2.19	.981			
	54	4.25	22.1	2.93	.992			
	57	4.29	11.7	2.04	.982			
	58	4.28	38.6	1.07	.981			
	59	4.25	16.2	2.11	.989			
	60	4.21	11.9	1.89	.992			
	62	4.07	17.5	4.22	.998			
	63	4.07	20.9	1.89	.984	3.89	4.07	.999
	64	4.02	46.3	1.44	.996	5.65	6.67	.977
	65	3.97	17.5	2.45	.994	2.15	16.7	.980

APPENDIX III

Tabulation of samples used.

Series	Side 1	Side 2
36	P2	P3
37	P2	P1
43	Pb1	P1
44	Pb1	P5
47	P7	Pb3
48	P8	Pb2
49	P8	Cd1
52	P8	Cd2
54 ($KCl:Pb^{2+}$-H_2O Experiment)	P10	Pb4
56 ($KCl:Cd^{2+}$-Atmo. H_2O Experiment)	P10	Cd3